

Robust Preference Optimization with Provable Noise Tolerance for LLMs

Xize Liang^{1,2†} Chao Chen² Jie Wang^{1‡} Yue Wu² Zhihang Fu² Zhihao Shi^{1,2} Feng Wu¹ Jieping Ye²

Abstract

The preference alignment aims to enable large language models (LLMs) to generate responses that conform to human values, which is essential for developing general AI systems. Ranking-based methods—a promising class of alignment approaches—learn human preferences from datasets containing response pairs by optimizing the log-likelihood margins between preferred and dis-preferred responses. However, due to the inherent differences in annotators’ preferences, ranking labels of comparisons for response pairs are unavoidably noisy. This seriously hurts the reliability of existing ranking-based methods. To address this problem, we propose a provably noise-tolerant preference alignment method, namely **RO**bstust **P**reference **O**ptimization (ROPO). To the best of our knowledge, ROPO is the *first* preference alignment method with noise-tolerance guarantees. The key idea of ROPO is to dynamically assign conservative gradient weights to response pairs with high label uncertainty, based on the log-likelihood margins between the responses. By effectively suppressing the gradients of noisy samples, our weighting strategy ensures that the expected risk has the same gradient direction independent of the presence and proportion of noise. Experiments on three open-ended text generation tasks with four base models ranging in size from 2.8B to 13B demonstrate that ROPO significantly outperforms existing ranking-based methods.

1. Introduction

The preference alignment has been substantiated as a pivotal source of the astonishing ability of large language models (LLMs) to understand various queries and provide responses

[†]Work done during Xize Liang’s research internship at Alibaba Cloud. Email: xizeliang@mail.ustc.edu.cn. [‡]Corresponding author. ¹Department of Electronic Engineering and Information Science, University of Science and Technology of China, Hefei, China ²Alibaba Cloud, Hangzhou, China. Correspondence to: Jie Wang <jiewangx@ustc.edu.cn>.



Figure 1. The inter-annotator agreement between human annotators and LLMs on the Reddit TL;DR dataset (Völske et al., 2017; Stiennon et al., 2020). The “Label”, “Llama”, and “Qwen” refer to the labels in the dataset, Llama-2-70B, and Qwen-Max, respectively. For details about Llama-2-70B and Qwen-Max, please refer to Appendix A.3. We assess the preferences of human annotators across 200 response pairs and extend the evaluation to 1,000 pairs for LLMs, which include the initial 200 pairs.

that align with human expectations (Wang et al., 2023c; Bubeck et al., 2023; Lin et al., 2023; Achiam et al., 2023). A typical approach of preference alignment is Reinforcement Learning from Human Feedback (RLHF) (Casper et al., 2023; Ziegler et al., 2019), which first trains a reward model to fit human preferences and then runs an RL algorithm (Schulman et al., 2017) to steer LLMs towards producing high-reward responses. However, it is widely recognized that RLHF may suffer from the misgeneralized reward modeling (Casper et al., 2023) and the unstable training of RL (Liu et al., 2023) in real-world applications (Shen et al., 2023; Rafailov et al., 2023; Wu et al., 2023).

To address these problems, various ranking-based preference alignment methods bypass the explicit reward modeling stage and do not use RL techniques (Rafailov et al., 2023; Yuan et al., 2023a; Wang et al., 2023a; Song et al., 2023). Specifically, they directly learn human preferences from datasets containing response pairs by optimizing the log-likelihood margins between preferred and dis-preferred responses. Owing to the stable and computa-

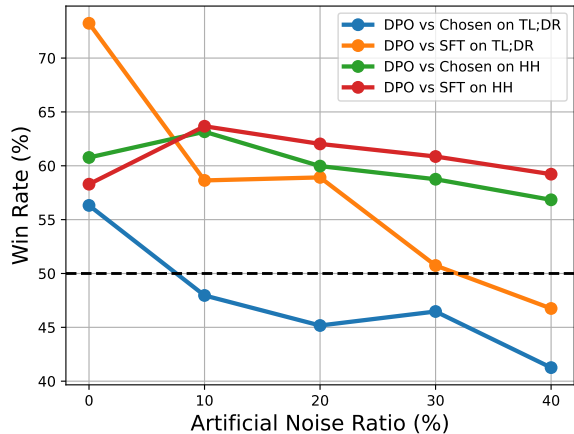


Figure 2. The label noise greatly affects the win rate of DPO (Rafailov et al., 2023) against the chosen responses and the SFT model on the Anthropic-HH (Bai et al., 2022) and TL:DR (Völske et al., 2017; Stiennon et al., 2020) datasets. The artificial noise originates from our alteration of labels in a portion of the dataset.

tionally lightweight supervised learning paradigm, ranking-based methods have emerged as competitive alternatives to RLHF, thus drawing increasing attention recently (Shen et al., 2023; Wang et al., 2023c).

Although impressive, ranking-based methods are heavily dependent on the high-quality preference ranking data, which is costly and limited in practice (Kim et al., 2023; Chen et al., 2024). First, the noise (e.g., incorrect or ambiguous preferences) in the preference ranking data is inevitable (Wang et al., 2024), whether the annotators are humans or LLMs. Figure 1 reports the inter-annotator agreement across different humans and LLMs. The data indicates that the agreement lies within a relatively low range of 57%-76%, reflecting an approximate noise proportion of 25%-45%. Second, existing ranking-based methods are sensitive to the noise in the preference data. As shown in Figure 2, we observe a significant change in the performance of Direct Preference Optimization (DPO) (Rafailov et al., 2023), a representative ranking-based method, as the noise ratio increases. Specifically, the performance decreases greatly under even 10% noisy labels. Therefore, it is highly desirable to develop a noise-tolerant preference alignment method.

In this paper, we propose a provably noise-tolerant method, namely **RO**bst **P**reference **O**ptimization (ROPO), to mitigate the adverse effects of the label noise on the preference alignment. The key idea of ROPO is to dynamically assign conservative gradient weights to response pairs with high label uncertainty. Specifically, our ROPO’s gradient weighting function is an even function with respect to the log-likelihood margin between the responses, as shown in Figure 3. For a response pair, the more the log-likelihood margin’s value diverges from the preference label, the greater the un-

certainty ROPO attributes to the label, and consequently, the smaller the gradient weight ROPO assigns. Our weighting strategy not only effectively suppresses the gradient magnitudes of noisy samples, but its symmetry also ensures that the expected risk maintains the same gradient direction under both noisy and noise-free conditions. We summarize our main contributions as follows.

- We propose the *first* provably noise-tolerant preference alignment method, namely ROPO, to the best of our knowledge.
- We show that the expected risk of our ROPO objective under a noisy preference distribution shares the same optimal solution with that under the noise-free preference distribution, under mild assumptions and *without needing to know the noise ratio*.
- We conduct experiments on three open-ended text generation tasks with four base models ranging in size from 2.8B to 13B. The results demonstrate that ROPO outperforms existing ranking-based alignment methods by a large margin.

2. Related Work

Preference Alignment of LLMs. Preference learning-based alignment has recently propelled substantial advancements in LLMs, revealing remarkable capabilities (Bubeck et al., 2023; Lin et al., 2023). The most representative paradigm of preference alignment is Reinforcement Learning from Human Feedback (RLHF) (Ziegler et al., 2019; Ouyang et al., 2022), which involves training a reward model to capture human preferences and then steering LLMs towards producing high-reward responses through RL algorithms, such as Proximal Policy Optimization (PPO) (Schulman et al., 2017). However, in real applications, RL-based methods are complex and prone to instability during training (Rafailov et al., 2023; Wu et al., 2023; Yuan et al., 2023a). Therefore, many recent studies have explored more straightforward and stable alternatives for RLHF (Yuan et al., 2023b; Rafailov et al., 2023; Song et al., 2023; Wang et al., 2023b; Lin et al., 2023; Li et al., 2023; Wang et al., 2023c; Zhao et al., 2022). Among these studies, the most promising direction is to use a contrastive or ranking loss to calibrate the likelihood of the output sequence. Specifically, RRHF (Yuan et al., 2023b) introduces a ranking loss to encourage larger likelihoods for better responses and smaller likelihoods for worse responses. Sequence Likelihood Calibration (SLiC) (Zhao et al., 2022) uses a spectrum of calibration losses to align the model’s outputs with reference sequences in the model’s latent space. Besides, another important work is DPO (Rafailov et al., 2023), which implicitly optimizes the same objective as existing RLHF-based methods and enables human preference alignment directly with a simple cross-entropy loss.

Although recent ranking-based alignment methods are user-friendly and have shown promising performance over RL-based approaches, they heavily rely on a substantial volume of high-quality preference data, which is costly to annotate and not always accessible. This paper provides a practical alternative solution, which enables effective preference alignment even with noisy preference data.

Learning from Noisy Data. In the era of deep learning and LLMs, there is an urgent demand for large-scale training samples, and the cost of manually annotating or filtering data is often prohibitively expensive in most circumstances (Song et al., 2022). Therefore, techniques for learning from noise data have becoming increasingly important, which primarily fall into three categories. The first category is sample-selection based methods (Swayamdipta et al., 2020; Pleiss et al., 2020; Paul et al., 2021; Sorscher et al., 2022), which identify high-quality samples before training and prune away the noisy or valueless samples. For example, Swayamdipta et al. (2020) use the training dynamics to identify valuable samples, and Paul et al. (2021) propose to assign a score to each sample based on the norm of its expected loss gradient early in the training stage. The second category is weighting-based methods, which assign greater weights for important samples and lesser weights for noisy samples within the loss function (Ren et al., 2018; Han et al., 2022; Shu et al., 2019). Besides, another important area of research is dedicated to the design of loss functions that are robust to noise (Ghosh et al., 2017a; Wang et al., 2019; Zhang & Sabuncu, 2018). The findings in (Ghosh et al., 2017a) indicate that the traditional cross-entropy loss is sensitive to the label noise, while symmetric loss functions are robust to such noise. Furthermore, recent advances in LLMs have also underscored the essential role of data quality in both pre-training and supervised fine-tuning (SFT) phases of LLMs (Marion et al., 2023; Zhou et al., 2023; Korbak et al., 2023). However, to the best of our knowledge, the exploration of robust preference alignment with noisy data remains an untouched territory. In this paper, we propose a noise-tolerant preference alignment method.

3. Problem Setting and Preliminaries

Denote an LLM with parameters θ as π_θ . Given a query or prompt in the form of a sequence $\mathbf{x} = [x_1, \dots, x_n]$, the model generates a response $\mathbf{y} = [y_1, \dots, y_m]$, where the tokens $(x_i)_{i=1}^n$ and $(y_j)_{j=1}^m$ come from a predefined vocabulary. LLM generates responses in an autoregressive paradigm. Specifically, the model samples y_j from the conditional probability distribution $\pi_\theta(\cdot | \mathbf{x}, \mathbf{y}_{1:j-1})$, where $\mathbf{y}_{1:0}$ is null and $\mathbf{y}_{1:j-1} = [y_1, \dots, y_{j-1}]$ for $j = 2, \dots, m$. Finally, we can decompose the conditional probability $\pi_\theta(\mathbf{y} | \mathbf{x})$ into

$$\pi_\theta(\mathbf{y} | \mathbf{x}) = \prod_{j=1}^m \pi_\theta(y_j | \mathbf{x}, \mathbf{y}_{1:j-1}). \quad (1)$$

3.1. Preference Alignment

The preference alignment aims at training LLM to generate responses that conform to human values and expectations, such as being helpful, harmless, and honest (Askell et al., 2021). Existing preference alignment frameworks consist of two main stages: (1) supervised fine-tuning (SFT) and (2) preference learning.

Supervised Fine-Tuning. During the SFT phase, we fine-tune a pretrained model on high-quality datasets of downstream tasks (e.g., dialogue and post summarization) via maximum likelihood, in order to teach the model to respond to queries. We denote the supervised fine-tuned model π_{sft} .

Preference Learning. During the preference learning phase, we train the model π_θ (initialized by π_{sft}) based on human preference data to achieve the ultimate goal of preference alignment. Specifically, an entry of preference data contains a query \mathbf{x} , two responses \mathbf{y}_1 and \mathbf{y}_2 , and a preference ranking label c provided by a human annotator. We use $c = 0$ to indicate that \mathbf{y}_1 is preferred to \mathbf{y}_2 (denoted $\mathbf{y}_1 \succ \mathbf{y}_2 | \mathbf{x}$) and use $c = 1$ to indicate the opposite. We assume the preference data $(\mathbf{x}, \mathbf{y}_1, \mathbf{y}_2, c)$ are sampled from a distribution \mathcal{D} . As we state in Section 1, reliably labeling data in practice is very costly in the context of preference learning.

A popular theoretical formulation of the generative process of the preference label given the query and responses is the Bradley-Terry (BT) model (Bradley & Terry, 1952), i.e.,

$$P^*(\mathbf{y}_1 \succ \mathbf{y}_2 | \mathbf{x}) = \sigma\left(r^*(\mathbf{y}_1, \mathbf{x}) - r^*(\mathbf{y}_2, \mathbf{x})\right), \quad (2)$$

where σ is the sigmoid function and r^* is a latent reward distribution over responses. Because r^* and P^* are inaccessible, the key step in existing preference learning methods is to explicitly or implicitly approximate r^* and P^* .

RLHF (Ouyang et al., 2022) replaces r^* in Eq. (2) with a parameterized reward model r_ϕ to obtain the estimated preference distribution P_ϕ , and train r_ϕ via maximum likelihood on preference data. Then, RLHF uses the well-trained r_ϕ to provide signal for the reinforcement learning of the language model. Note that RLHF does not directly use the preference ranking data to train the language model.

Due to the complexity and instability of RLHF, some recent works (Rafailov et al., 2023; Azar et al., 2023; Wang et al., 2023a) directly use the ranking information in the preference data to train language models. Their core idea is to maximize the margin between the log-likelihood of preferred and dis-preferred responses. For example, the objectives of direct preference optimization (DPO) (Rafailov et al., 2023) is given by

$$\ell_{\text{dpo}} = -\log \sigma\left(\beta \log \frac{\pi_\theta(\mathbf{y}_1 | \mathbf{x})}{\pi_{\text{sft}}(\mathbf{y}_1 | \mathbf{x})} - \beta \log \frac{\pi_\theta(\mathbf{y}_2 | \mathbf{x})}{\pi_{\text{sft}}(\mathbf{y}_2 | \mathbf{x})}\right), \quad (3)$$

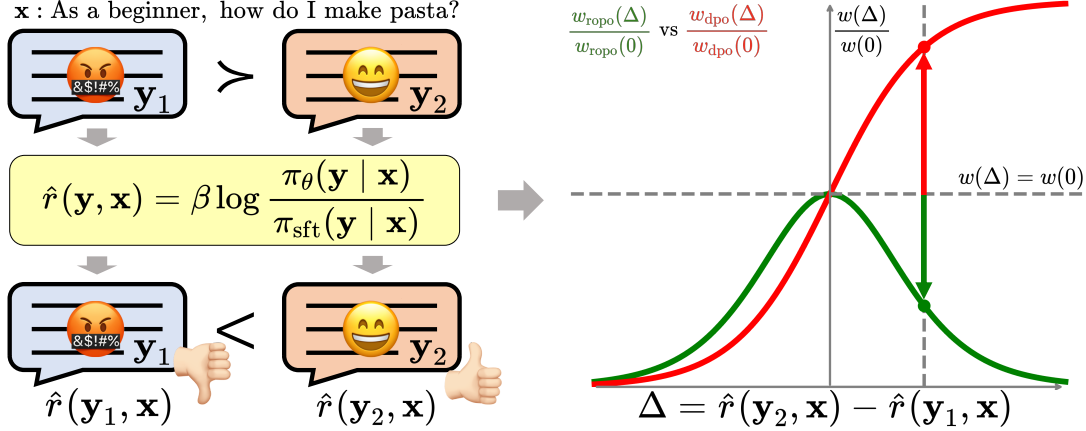


Figure 3. A comparison of the gradient weights assigned by ROPO and DPO (Rafailov et al., 2023) to a noisy preference sample $(\mathbf{x}, \mathbf{y}_1, \mathbf{y}_2, \hat{c} = 0)$. We denote the margin between the log-likelihood rewards of \mathbf{y}_2 and \mathbf{y}_1 by $\Delta = \hat{r}(\mathbf{y}_2, \mathbf{x}) - \hat{r}(\mathbf{y}_1, \mathbf{x})$. In the right-hand side, the green and red curves represent the graphs of $w_{\text{ropo}}(\Delta)/w_{\text{ropo}}(0)$ and $w_{\text{dpo}}(\Delta)/w_{\text{dpo}}(0)$, respectively. Note that $w(0)$ is the weight when $\hat{r}(\mathbf{y}_1, \mathbf{x}) = \hat{r}(\mathbf{y}_2, \mathbf{x})$, so the curve lying above $w(\Delta) = w(0)$ represents amplifying the magnitude of the gradient.

where β is a hyperparameter. Ranking-based methods are more computationally lightweight and stable than RLHF, thus have drawn increasing attention recently. Therefore, we mainly focus on ranking-based methods in this paper.

3.2. Preference Learning with Noisy Data

Due to the inherent differences among the preferences of different annotators, preference ranking labels are unavoidably noisy. This seriously affects the reliability of existing ranking-based methods. Therefore, it is important to study the preference learning with noisy data.

In this setting, we have no access to the clean dataset, denoted $D = \{(\mathbf{x}^{(i)}, \mathbf{y}_1^{(i)}, \mathbf{y}_2^{(i)}, c^{(i)})\}_{i=1}^N$, which is drawn from a distribution \mathcal{D} . Instead, we can only obtain a noisy dataset $D_{\eta} = \{(\mathbf{x}^{(i)}, \mathbf{y}_1^{(i)}, \mathbf{y}_2^{(i)}, \hat{c}^{(i)})\}_{i=1}^N$ drawn from a distribution \mathcal{D}_{η} , where

$$\hat{c}^{(i)} = \begin{cases} c^{(i)} & \text{with probability } (1 - \eta), \\ 1 - c^{(i)} & \text{with probability } \eta. \end{cases}$$

Suppose that a ranking-based method employs a loss function ℓ and finds the optimal solutions θ^* and θ_{η}^* by solving

$$\theta^* = \arg \min_{\theta} \mathbb{E}_{(\mathbf{x}, \mathbf{y}_1, \mathbf{y}_2, c) \sim \mathcal{D}} [\ell(\theta; \mathbf{x}, \mathbf{y}_1, \mathbf{y}_2, c, \pi_{\theta})] \quad (4)$$

and

$$\theta_{\eta}^* = \arg \min_{\theta} \mathbb{E}_{(\mathbf{x}, \mathbf{y}_1, \mathbf{y}_2, \hat{c}) \sim \mathcal{D}_{\eta}} [\ell(\theta; \mathbf{x}, \mathbf{y}_1, \mathbf{y}_2, \hat{c}, \pi_{\theta})], \quad (5)$$

We hope that our method satisfies $\theta_{\eta}^* = \theta^*$, that is, the optimal solution it obtains is not affected by the noise. Following the definition in (Ghosh et al., 2017b), if $\theta^* = \theta_{\eta}^*$

under mild assumptions (such as $\eta < 50\%$), we say that the ranking-based method is *noise-tolerant* or *noise-robust*.

4. Robust Preference Optimization

We first intuitively illustrate that existing ranking-based methods such as DPO is sensitive to noisy labels in Section 4.1. Then, we propose a noise-robust loss function for preference learning in Section 4.2, and following with a theoretical analysis of our method in Section 4.3. In this section, we discuss the case when $\hat{c} = 0$, i.e., $\mathbf{y}_1 \succ \mathbf{y}_2 | \mathbf{x}$, unless otherwise stated. The case when $\hat{c} = 1$ is analogous.

4.1. DPO is Sensitive to Noise

Given a noisy preference sample $(\mathbf{x}, \mathbf{y}_1, \mathbf{y}_2, \hat{c} = 0)$, according to (Rafailov et al., 2023), the gradient of the DPO loss in Eq. (3) is given by

$$\begin{aligned} \nabla_{\theta} \ell_{\text{dpo}} &= -\beta \sigma(\hat{r}(\mathbf{y}_2, \mathbf{x}) - \hat{r}(\mathbf{y}_1, \mathbf{x})) \cdot \nabla \log \frac{\pi_{\theta}(\mathbf{y}_1 | \mathbf{x})}{\pi_{\theta}(\mathbf{y}_2 | \mathbf{x})} \\ &\triangleq -w_{\text{dpo}}(\mathbf{x}, \mathbf{y}_1, \mathbf{y}_2) \cdot \nabla \log \frac{\pi_{\theta}(\mathbf{y}_1 | \mathbf{x})}{\pi_{\theta}(\mathbf{y}_2 | \mathbf{x})}, \end{aligned} \quad (6)$$

where $\hat{r}(\mathbf{y}, \mathbf{x}) = \beta \log \frac{\pi_{\theta}(\mathbf{y} | \mathbf{x})}{\pi_{\text{sft}}(\mathbf{y} | \mathbf{x})}$ is the log-likelihood reward function of DPO. The gradient of the DPO loss increases the log-likelihood of \mathbf{y}_1 and decreases the log-likelihood of \mathbf{y}_2 . Intuitively, the greater the discrepancy between the reward function's comparison of \mathbf{y}_1 and \mathbf{y}_2 and the label $\mathbf{y}_1 \succ \mathbf{y}_2 | \mathbf{x}$, the greater the weight $w_{\text{dpo}}(\mathbf{x}, \mathbf{y}_1, \mathbf{y}_2)$ of the DPO gradient becomes.

However, if the label is incorrect, i.e., the ground truth label is $\mathbf{y}_2 \succ \mathbf{y}_1 | \mathbf{x}$, the weight of the DPO gradient may further amplify the negative impact of the noise on the preference

training because the sigmoid function is monotonically increasing, as shown in Figure 3.

To address this problem, we propose a gradient weighting technique that suppresses the gradient of potentially noisy samples. An appealing feature of the weighting technique is that it leads to a *provable noise-tolerant* preference learning objective, as shown in Section 4.3.

4.2. Noise Tolerant Gradient Weighting

Our key idea is simple and straightforward: when the margin between the log-likelihood rewards of \mathbf{y}_2 and \mathbf{y}_1 , i.e., $\hat{r}(\mathbf{y}_2, \mathbf{x}) - \hat{r}(\mathbf{y}_1, \mathbf{x})$, is excessively positive, we should assign a conservative weight to the gradient. The intuition behind this is that when the log-likelihood reward of \mathbf{y}_2 is much higher than that of \mathbf{y}_1 , we speculate that the model has a high uncertainty about the label $\mathbf{y}_1 \succ \mathbf{y}_2 \mid \mathbf{x}$. Based on this idea, we propose the conservative gradient weight

$$\begin{aligned} w_{\text{ropo}} &= \sigma(\hat{r}(\mathbf{y}_1, \mathbf{x}) - \hat{r}(\mathbf{y}_2, \mathbf{x})) w_{\text{dpo}} \\ &= \beta \sigma(\hat{r}(\mathbf{y}_2, \mathbf{x}) - \hat{r}(\mathbf{y}_1, \mathbf{x})) \sigma(\hat{r}(\mathbf{y}_1, \mathbf{x}) - \hat{r}(\mathbf{y}_2, \mathbf{x})) \end{aligned} \quad (7)$$

As illustrated in Figure 3, the gradient weight w_{ropo} is designed as a symmetric function that decreases as the absolute value of the reward margin between \mathbf{y}_1 and \mathbf{y}_2 increases.

Then, the weighted gradient is

$$\begin{aligned} &\nabla_{\theta} \ell_{\text{ropo}} \\ &= -w_{\text{ropo}} \cdot \nabla \log \frac{\pi_{\theta}(\mathbf{y}_1 \mid \mathbf{x})}{\pi_{\theta}(\mathbf{y}_2 \mid \mathbf{x})} \\ &= -\beta \sigma \left(\beta \log \frac{\pi_{\theta}(\mathbf{y}_2 \mid \mathbf{x})}{\pi_{\text{sft}}(\mathbf{y}_2 \mid \mathbf{x})} - \beta \log \frac{\pi_{\theta}(\mathbf{y}_1 \mid \mathbf{x})}{\pi_{\text{sft}}(\mathbf{y}_1 \mid \mathbf{x})} \right) \\ &\quad \cdot \sigma \left(\beta \log \frac{\pi_{\theta}(\mathbf{y}_1 \mid \mathbf{x})}{\pi_{\text{sft}}(\mathbf{y}_1 \mid \mathbf{x})} - \beta \log \frac{\pi_{\theta}(\mathbf{y}_2 \mid \mathbf{x})}{\pi_{\text{sft}}(\mathbf{y}_2 \mid \mathbf{x})} \right) \\ &\quad \cdot \nabla \log \frac{\pi_{\theta}(\mathbf{y}_1 \mid \mathbf{x})}{\pi_{\theta}(\mathbf{y}_2 \mid \mathbf{x})}. \end{aligned} \quad (8)$$

Hence, the corresponding objective, which we name the ROBust Preference Optimization (ROPO) loss, is

$$\begin{aligned} \ell_{\text{ropo}} &= \int \nabla_{\theta} \ell_{\text{ropo}} d\theta \\ &= \sigma \left(\beta \log \frac{\pi_{\theta}(\mathbf{y}_2 \mid \mathbf{x})}{\pi_{\text{sft}}(\mathbf{y}_2 \mid \mathbf{x})} - \beta \log \frac{\pi_{\theta}(\mathbf{y}_1 \mid \mathbf{x})}{\pi_{\text{sft}}(\mathbf{y}_1 \mid \mathbf{x})} \right), \end{aligned} \quad (9)$$

where we omit the constant term of the primitive function (see Appendix B.1 for the detailed derivation).

Compared to the DPO loss, the introduced ROPO loss is more robust to noisy samples as it assigns conservative gradient weights for the sample with high uncertainty. However,

the ROPO loss may also potentially curb the model’s performance on clean preference dataset. Therefore, in practice, we are able to combine the DPO loss and ROPO loss to obtain the best trade-off between radical and conservative gradient magnitude, which leads to further improvement. The final loss can be given as

$$\ell = \alpha \ell_{\text{ropo}} + \gamma \ell_{\text{dpo}}, \quad (10)$$

where α and γ are trade-off hyperparameters.

4.3. Theoretical Analysis

In this section, we provide the theoretical analysis of the noise-tolerance of ROPO. Theorem 4.1 shows that under mild and standard assumptions, the expected risk of the ROPO objective under a noisy preference data distribution shares the same optimal solution with that under the clean preference data distribution.

Theorem 4.1. *Assume that each entry of preference data has a probability of $\eta_0 < \frac{1}{2}$ of being labeled incorrectly, then ℓ_{ropo} is noise-tolerant, while the objectives of DPO (Rafailov et al., 2023) and IPO (Azar et al., 2023) are not.*

Proof. Please refer to Appendix B.2. \square

4.4. Connections to Traditional Noise-tolerant Losses

Aligning LLMs with noisy preference data remains unexplored, while many noise-tolerant loss functions have already been proposed in the traditional field of machine learning. Some representative noise-tolerant losses include unhinged loss (Van Rooyen et al., 2015), symmetric cross-entropy and MAE loss (reverse cross-entropy) (Wang et al., 2019), normalized cross-entropy (Ma et al., 2020), and asymmetric loss class (Zhou et al., 2021). The noise-tolerance of the first three losses stems from the symmetric condition (Ghosh et al., 2017a) they satisfy, i.e., $\sum_{i=1}^k \ell(\theta; \mathbf{z}, i) = C$ for any sample \mathbf{z} , where $\ell(\theta; \mathbf{z}, i)$ is the loss when \mathbf{z} is classified to the class i and C is a constant. Zhou et al. (2021) further relaxes the symmetric condition to the asymmetric condition, leading to a class of asymmetric loss functions that are tolerant to various types of noise.

Our ROPO loss adheres the symmetric condition and is formally equivalent to the unhinged loss and MAE loss. Specifically, if we interpret the right hand side of Eq. (9) as $P_{\theta}(\mathbf{y}_2 \succ \mathbf{y}_1 \mid \mathbf{x})$ —the likelihood that \mathbf{y}_2 is preferred to \mathbf{y}_1 given \mathbf{x} , our ROPO loss is indeed $1 - P_{\theta}(\mathbf{y}_1 \succ \mathbf{y}_2 \mid \mathbf{x})$, which resembles the unhinged loss and MAE loss. Apart from being an objective obtained by integrating the gradient with a symmetric conservative weight, this is another perspective on our ROPO loss and also explains why the ROPO loss exhibits provable noise-tolerance. Besides, our combination of ℓ_{ropo} (MAE loss) and ℓ_{dpo} (cross-entropy) in Eq.

Table 1. Win rates (%) of **different methods against SFT models** under different artificial noise ratios. The bold font indicates the best result and an underline indicates the second-best result.

Dataset	Method	Artificial noise ratio (%)				
		0	10	20	30	40
TL;DR	DPO	<u>73.23</u>	58.63	58.90	50.73	46.74
	IPO	59.93	40.89	45.34	42.00	41.07
	C-DPO	69.68	56.12	52.03	46.83	49.25
	C-IPO	52.87	<u>71.93</u>	<u>65.71</u>	<u>61.04</u>	<u>53.15</u>
	ROPO	82.33	82.15	79.36	78.69	71.19
HH	DPO	58.29	<u>62.50</u>	<u>61.15</u>	<u>60.85</u>	59.21
	IPO	59.35	59.74	56.59	59.40	55.56
	C-DPO	61.19	62.16	58.93	59.41	55.61
	C-IPO	<u>61.66</u>	59.49	58.99	58.37	<u>59.26</u>
	ROPO	61.94	62.51	61.33	62.33	60.44

(10) mirrors the structure of the symmetric cross-entropy, offering insight into the superior empirical performance of ROPO on noisy data, as shown in Section 5.

5. Experiments

5.1. Experimental Settings

Tasks and Datasets. We evaluate ROPO on three open-ended text generation datasets, i.e., the Reddit TL;DR summarization dataset (Völske et al., 2017; Stiennon et al., 2020), the Anthropic Helpful and Harmless (HH) dialogue dataset (Bai et al., 2022), and the Human ChatGPT Comparison Corpus (HC3) dataset (Guo et al., 2023). Due to space limitations, in the main text, we only show the results on TL;DR and HH. For results on the HC3 dataset, please refer to Appendix C.1.

In the TL;DR dataset, the queries are forum posts from Reddit, and the task is to generate summaries of the key points of the posts. In the HH dataset, each prompt is a conversation with historical information between a human and an AI assistant, ending with “Assistant:”. The task is to generate helpful, engaging, and harmless responses.

To construct datasets with various artificial noise ratios, we randomly alter preference labels at different proportions within the three datasets (See Section 5.2). For more details about the datasets, please refer to Appendix A.1. We run all experiments on eight NVIDIA A100 GPUs (80 GB).

Baselines and Models. Our preference alignment baselines include the SFT model, DPO (Rafailov et al., 2023), and IPO (Azar et al., 2023). As the label smoothing technique has been explored to improve the noise robustness of DPO¹, we also compare ROPO with the conservative variants of DPO and IPO combined with the label smoothing, termed

¹<https://ericmitchell.ai/cdpo.pdf>

as C-DPO and C-IPO. For their objectives, please refer to Appendix A.2.

Following (Rafailov et al., 2023), we use a fine-tuned GPT-J-6B² as the SFT model on TL;DR; whereas on the HH dataset, we fine-tune a Pythia-2.8B (Biderman et al., 2023) model on only the preferred responses to form the SFT model. For more information, please refer to Appendix A.2.

To test the effectiveness of ROPO on models of various sizes, we use the popular Llama-2-7B and Llama-2-13B (Touvron et al., 2023) as base models for the preference alignment, and show the results in Appendix C.1.

In practice, the data used for SFT may also contain noise, and this coupled with the noise in the preference data may have a greater negative impact on the preference alignment than if there is only noise in the preference data. To test the performance of ROPO in this situation, we conduct experiments on HH with SFT models trained on noisy data. The results are shown in Appendix C.2.

Evaluation. To evaluate the noise-robustness of ROPO and baselines, we compare the responses of models trained under different noise ratios with those of SFT models that have not been exposed to noisy labels. Furthermore, we compare the responses of ROPO with those of baselines to directly illustrate the distinctions between ROPO and baselines.

Following (Rafailov et al., 2023), we employ large language models as referees to conduct head-to-head comparisons, using the win rate as the evaluation metric to assess ROPO against baselines. The win rate can be computed as

$$\rho = \frac{\#(\text{Win}) + \#(\text{Tie})/2}{\#(\text{Comparisons})},$$

where $\#(\text{Win})$, $\#(\text{Tie})$, and $\#(\text{Comparisons})$ are the numbers of wins, ties, and comparisons.

Due to the high inference expense and sluggish response time of GPT-4, we employ the more affordable yet powerful Qwen-Max as the referee. It is worth noting that Qwen-Max is the highest-ranked large model with a free API on the CompassRank leaderboard³, as of the submission of this paper. We also verify the consistency between the judgements of human, Qwen-Max, and GPT-4 in Section 5.4 to justify our usage of Qwen-Max for evaluation. For more information about Qwen-Max and the evaluation, please refer to Appendix A.3.

²https://huggingface.co/CarperAI/openai_summarize_tldr_sft

³<https://rank.opencompass.org.cn/home>

Table 2. Win rates (%) of **ROPO** against baselines under different artificial noise ratios.

Dataset	Baseline	Artificial noise ratio (%)				
		0	10	20	30	40
TL;DR	DPO	76.94	79.80	81.03	78.99	72.67
	IPO	82.33	84.37	79.54	81.40	73.04
	C-DPO	72.86	77.32	78.24	77.13	69.89
	C-IPO	79.36	69.68	74.53	75.46	70.33
HH	DPO	51.87	51.43	53.40	53.63	54.91
	IPO	56.30	58.09	60.53	61.88	58.70
	C-DPO	50.73	52.15	59.25	57.53	60.53
	C-IPO	55.65	59.62	59.62	57.12	53.26

5.2. ROPO is Robust to Label Noise

In this section, we evaluate the robustness of ROPO to the label noise on the TL;DR and HH datasets. The noisy dataset is constructed by randomly alter the labels of 10% to 40% of the training data in both datasets.

After being fine-tuned with ROPO or baseline methods, the models generate responses to queries in the test split of the two datasets at a temperature of 0 to ensure the reproducibility of the results. Then, we compare the responses produced by different methods with those of the SFT models, which have not been exposed to noisy labels. We present the win rates of different methods against the SFT models under different noise ratios in Table 1.

We can make several interesting observations from the table as follows. (1) For all preference alignment methods, their win rates show a decreasing trend as the noise ratio increases. (2) Compared to the competitors, our proposed ROPO demonstrates more stable performance under noisy preference data. Specifically, the win rate of ROPO drops by 2.97% under 20% noisy labels, while both DPO and IPO drop by at least 14%. (3) ROPO consistently outperforms the baselines under different noise ratios in both TL;DR and HH datasets. Even without artificial noise, ROPO still exceeds DPO by 9.10% on TL;DR, which indicates that this dataset inherently includes a significant amount of noise. (4) On the HH dataset, the performance is less sensitive to label noise, and the improvement of ROPO over baselines is less significant than on the TL;DR dataset. We attribute the reason to the fact that the SFT model has been initially aligned on the same preference distribution, and there is limited room for further improvement on this basis.

Furthermore, we also conduct a direct comparison of the response quality between ROPO and baseline methods, presenting the win rates in Table 2. The results indicate that: (1) On both datasets, the win rate of ROPO consistently exceeds 50%, which demonstrates the superiority of ROPO. In particular, on the TL;DR dataset, the minimum win rate is 69% across different noise ratios, and at least 75% when

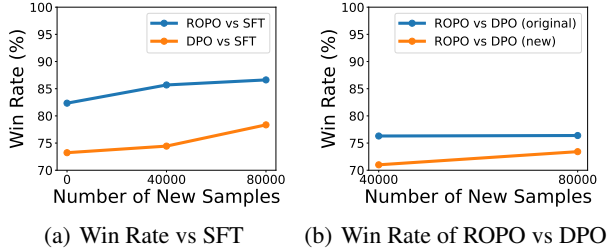


Figure 4. The win rate w.r.t. the number of new LLM-annotated samples. (a) The win rate of ROPO and DPO against the SFT model w.r.t. the number of new samples. (b) The win rate of ROPO against the model trained with DPO on the original dataset and the new mixed dataset w.r.t. the number of new samples.

the noise ratio is 30%. (2) The win rates against C-DPO and C-IPO are respectively smaller than those of DPO and IPO on the TL;DR dataset, demonstrating the effectiveness of applying the label smoothing technique. However, the effect of the label smoothing is unstable on HH, which is consistent with the conclusion illustrated in Table 1.

ROPO vs Label Smoothing. Based on the results presented in Table 1 and Table 2, we can conclude that the label smoothing contributes positively to improving the noise-robustness of the preference optimization. However, its impact is relatively modest when compared with the significant improvements yielded by our proposed ROPO. We attribute the superiority of ROPO to its dynamical assignment of conservative weights to the gradient of noisy samples, in contrast to the label smoothing, which only provides a constant change to the gradient weights. Specifically, the weights of the gradient $\nabla \log \frac{\pi_{\theta}(\mathbf{y}_1|\mathbf{x})}{\pi_{\theta}(\mathbf{y}_2|\mathbf{x})}$ assigned by C-DPO and C-IPO are respectively

$$w_{c-dpo} = w_{dpo} - \beta\varepsilon \quad \text{and} \quad w_{c-ipo} = w_{ipo} + \frac{2\varepsilon}{\beta}, \quad (11)$$

while the weight of ROPO is

$$w_{ropo} = w_{dpo} \cdot \sigma(\hat{r}(\mathbf{y}_1, \mathbf{x}) - \hat{r}(\mathbf{y}_2, \mathbf{x})). \quad (12)$$

5.3. Preference Alignment with LLM-Annotated Data

The application of LLM-annotated data for the preference alignment is an increasingly prevalent practice (Huang et al., 2023) and represents a critical scenario of applying the noise-robust preference learning. Therefore, in this section, we further explore the performance of ROPO in the scenario of using LLM-generated data for training. Specifically, in the first step, we use the SFT model of GPT-J-6B to generate 80,000 pairs of responses to the queries in the train split of TL;DR at a temperature of 1.0. Then, we generate preference labels of the LLM-generated responses with Qwen-Max, without having them checked by human annotators.

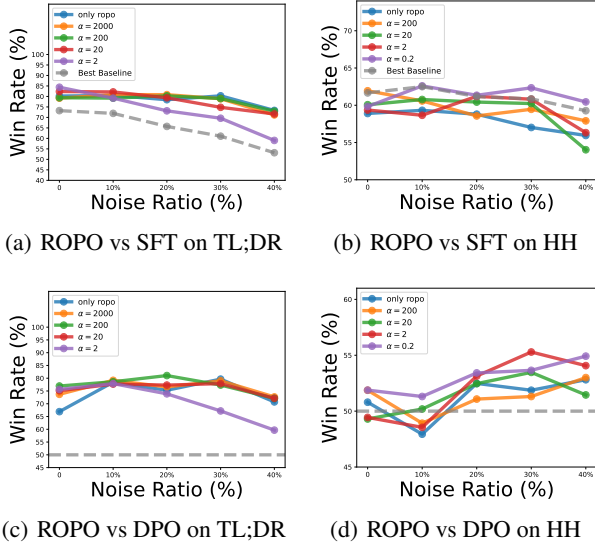


Figure 5. The win rate of ROPO with different hyperparameter α . Figures (a) and (b) show the win rate of ROPO against the SFT model on the TL;DR and HH datasets, respectively. The gray dotted line represents the win rate of the best-performing baseline method. Figures (c) and (d) show the win rate of ROPO against DPO on TL;DR and Anthropic, respectively. The gray dotted line indicates a win rate of 50%.

According to our experiment on the agreement evaluation of preferences in Figure 1, the preference labels generated by Qwen-Max inevitably carry some noise. Finally, we mix the generated noisy data into the original TL;DR dataset and train the SFT model on them with ROPO and DPO. We report the results in Figure 4.

As shown in Figure 4(a), the newly LLM-generated data brings improvements to both ROPO and DPO. Specifically, as the amount of newly generated data increases from 0 to 40,000 and then 80,000, the win rate of ROPO against the SFT model increases from 82.34% to 86.62%, and the win rate of DPO also increases from 73.23% to 78.35%. Although the two methods both have improved performance, ROPO still outperforms DPO by a large margin. Besides, we also conduct direct comparisons between ROPO and DPO, as shown in Figure 4(b). As the quantity of newly generated data increases, the win rate of ROPO against the DPO model trained on the original TL;DR dataset changes slightly, while that of ROPO against the DPO model trained on the newly constructed dataset increases by 2.42%. The result also indicates that our ROPO is more robust to the noisy samples introduced by LLM-generated data.

5.4. Ablation Studies

Sensitivity to Hyperparameters. To investigate the impact of the trade-off parameters α and γ , we conduct experiments

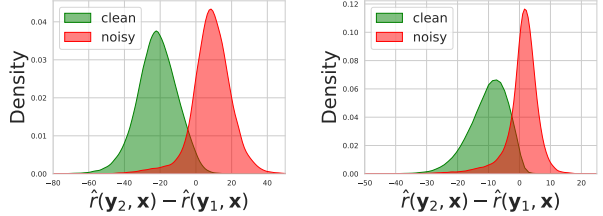


Figure 6. The distributions of margins between the log-likelihood rewards of y_2 and y_1 , i.e., $\hat{r}(y_2, x) - \hat{r}(y_1, x)$ after training for one epoch on HH at the noise ratio of (a) 20% and (b) 40%.

in two settings: (1) training only with the ROPO loss by setting $\gamma = 0$; (2) fixing $\gamma = 0.1$ and training models with different α . We conduct experiments on TL;DR and HH and present the results in Figure 5. As can be seen, our ROPO outperforms the best-performing baseline with most of trade-off parameters α across various noise ratios. Moreover, we notice that the model’s performance surpasses the best baseline in the most cases when trained solely with the ROPO loss, and incorporating the ROPO loss alongside DPO leads to further improvement in performance.

Distribution of Log-likelihood Reward Margin. The underlying intuition of ROPO is that if the model demonstrates a substantially larger log-likelihood reward for y_2 in comparison to y_1 , it implies that the model is highly uncertain about the preference label $y_1 \succ y_2 | x$. To verify this intuition, we compute the log-likelihood reward margins across clean and noisy samples after training the model on the Anthropic-HH dataset for one epoch. The results in Figure 6 demonstrate two important observations. The reward margins in the noisy data are significantly higher than that on the clean data, which confirms the soundness of our noise-tolerant gradient weighting. Moreover, we observe that the disparity between the two distributions diminishes as the noise ratio increases, which underscores the detrimental impact of noise on the preference learning.

GPT-4 and Human Evaluation. To verify the reliability of the results obtained using Qwen-Max as a referee, we engage GPT-4 and human annotators to evaluate a subset of the responses from the TL;DR dataset. Specifically, we initially randomly sample 500 queries from the test split of the TL;DR dataset, along with the corresponding responses generated by models trained with ROPO and DPO across various noise ratios. Then, we employ GPT-4 to conduct head-to-head comparisons between the responses from ROPO and DPO. Besides, we further select 100 queries from the initial set of 500 queries for the human evaluation. As shown in Table 3, the trends in the evaluation results of the three referees are highly consistent, and our ROPO outperforms DPO according to the judgement of all three

Table 3. Win rates (%) of **ROPO** against **DPO** evaluated by different referees under different noise ratios on the TL;DR dataset. #Samples denotes the number of samples for evaluation.

Referee	#Samples	Noise ratio (%)				
		0	10	20	30	40
Qwen-Max	4307	76.94	79.80	81.03	78.99	72.67
GPT-4	500	70.80	75.80	78.80	72.40	67.00
Human	100	71.00	—	81.00	—	80.00

referees, affirming that Qwen-Max serves as a reasonable surrogate for human and GPT-4 evaluations. For more details, please refer to Appendix A.3.

6. Conclusion

The presence of the noise in ranking labels is inherent and inevitable in the preference alignment of LLMs, and existing ranking-based methods are sensitive to the unavoidable noise. To address this problem, we propose a provably noise-tolerant preference alignment method, named Robust Preference Optimization (ROPO). To the best of our knowledge, ROPO is the first preference alignment method with provable noise-tolerance. ROPO dynamically assigns a conservative gradient weight to response pairs that exhibit a high degree of label uncertainty, based on the log-likelihood margin between the responses. Our weighting strategy mitigates the influence of noisy samples by suppressing their gradients, thus ensuring that the direction of the expected risk’s gradient remains the same, regardless of the presence and proportion of noise. Experiments on three open-ended text generation tasks with four base models ranging in size from 2.8B to 13B demonstrate that ROPO outperforms existing ranking-based methods by a large margin.

References

- Achiam, J., Adler, S., Agarwal, S., Ahmad, L., Akkaya, I., Aleman, F. L., Almeida, D., Altenschmidt, J., Altman, S., Anadkat, S., et al. Gpt-4 technical report. *arXiv preprint arXiv:2303.08774*, 2023.
- Askell, A., Bai, Y., Chen, A., Drain, D., Ganguli, D., Henighan, T., Jones, A., Joseph, N., Mann, B., DasSarma, N., et al. A general language assistant as a laboratory for alignment. *arXiv preprint arXiv:2112.00861*, 2021.
- Azar, M. G., Rowland, M., Piot, B., Guo, D., Calandriello, D., Valko, M., and Munos, R. A general theoretical paradigm to understand learning from human preferences. *arXiv preprint arXiv:2310.12036*, 2023.
- Bai, J., Bai, S., Chu, Y., Cui, Z., Dang, K., Deng, X., Fan, Y., Ge, W., Han, Y., Huang, F., et al. Qwen technical report. *arXiv preprint arXiv:2309.16609*, 2023.
- Bai, Y., Jones, A., Ndousse, K., Askell, A., Chen, A., DasSarma, N., Drain, D., Fort, S., Ganguli, D., Henighan, T., et al. Training a helpful and harmless assistant with reinforcement learning from human feedback. *arXiv preprint arXiv:2204.05862*, 2022.
- Biderman, S., Schoelkopf, H., Anthony, Q. G., Bradley, H., O’Brien, K., Hallahan, E., Khan, M. A., Purohit, S., Prashanth, U. S., Raff, E., et al. Pythia: A suite for analyzing large language models across training and scaling. In *International Conference on Machine Learning*, pp. 2397–2430. PMLR, 2023.
- Bradley, R. A. and Terry, M. E. Rank analysis of incomplete block designs: I. the method of paired comparisons. *Biometrika*, 39(3/4):324–345, 1952.
- Bubeck, S., Chandrasekaran, V., Eldan, R., Gehrke, J., Horvitz, E., Kamar, E., Lee, P., Lee, Y. T., Li, Y., Lundberg, S., et al. Sparks of artificial general intelligence: Early experiments with gpt-4. *arXiv preprint arXiv:2303.12712*, 2023.
- Casper, S., Davies, X., Shi, C., Gilbert, T. K., Scheurer, J., Rando, J., Freedman, R., Korbak, T., Lindner, D., Freire, P., et al. Open problems and fundamental limitations of reinforcement learning from human feedback. *arXiv preprint arXiv:2307.15217*, 2023.
- Chen, Z., Deng, Y., Yuan, H., Ji, K., and Gu, Q. Self-play fine-tuning converts weak language models to strong language models. *arXiv preprint arXiv:2401.01335*, 2024.
- Ghosh, A., Kumar, H., and Sastry, P. S. Robust loss functions under label noise for deep neural networks. In *Proceedings of the AAAI conference on artificial intelligence*, volume 31, 2017a.
- Ghosh, A., Kumar, H., and Sastry, P. S. Robust loss functions under label noise for deep neural networks. In *Proceedings of the AAAI conference on artificial intelligence*, volume 31, 2017b.
- Guo, B., Zhang, X., Wang, Z., Jiang, M., Nie, J., Ding, Y., Yue, J., and Wu, Y. How close is chatgpt to human experts? comparison corpus, evaluation, and detection. *arXiv preprint arxiv:2301.07597*, 2023.
- Han, Y., Pu, Y., Lai, Z., Wang, C., Song, S., Cao, J., Huang, W., Deng, C., and Huang, G. Learning to weight samples for dynamic early-exiting networks. In *European Conference on Computer Vision*, pp. 362–378. Springer, 2022.
- Huang, S., Zhao, J., Li, Y., and Wang, L. Learning preference model for llms via automatic preference data generation. In *Proceedings of the 2023 Conference on Empirical Methods in Natural Language Processing*, pp. 9187–9199, 2023.

- Kim, S., Bae, S., Shin, J., Kang, S., Kwak, D., Yoo, K. M., and Seo, M. Aligning large language models through synthetic feedback. *arXiv preprint arXiv:2305.13735*, 2023.
- Korbak, T., Shi, K., Chen, A., Bhalerao, R. V., Buckley, C., Phang, J., Bowman, S. R., and Perez, E. Pretraining language models with human preferences. In *International Conference on Machine Learning*, pp. 17506–17533. PMLR, 2023.
- Langley, P. Crafting papers on machine learning. In Langley, P. (ed.), *Proceedings of the 17th International Conference on Machine Learning (ICML 2000)*, pp. 1207–1216, Stanford, CA, 2000. Morgan Kaufmann.
- Li, Y., Wei, F., Zhao, J., Zhang, C., and Zhang, H. Rain: Your language models can align themselves without finetuning. *arXiv preprint arXiv:2309.07124*, 2023.
- Lin, B. Y., Ravichander, A., Lu, X., Dziri, N., Sclar, M., Chandu, K., Bhagavatula, C., and Choi, Y. The unlocking spell on base llms: Rethinking alignment via in-context learning. *arXiv preprint arXiv:2312.01552*, 2023.
- Liu, H., Sferrazza, C., and Abbeel, P. Chain of hindsight aligns language models with feedback. *arXiv preprint arXiv:2302.02676*, 2023.
- Ma, X., Huang, H., Wang, Y., Romano, S., Erfani, S., and Bailey, J. Normalized loss functions for deep learning with noisy labels. In *International conference on machine learning*, pp. 6543–6553. PMLR, 2020.
- Marion, M., Üstün, A., Pozzobon, L., Wang, A., Fadaee, M., and Hooker, S. When less is more: Investigating data pruning for pretraining llms at scale. *arXiv preprint arXiv:2309.04564*, 2023.
- Ouyang, L., Wu, J., Jiang, X., Almeida, D., Wainwright, C., Mishkin, P., Zhang, C., Agarwal, S., Slama, K., Ray, A., et al. Training language models to follow instructions with human feedback. *Advances in Neural Information Processing Systems*, 35:27730–27744, 2022.
- Paul, M., Ganguli, S., and Dziugaite, G. K. Deep learning on a data diet: Finding important examples early in training. *Advances in Neural Information Processing Systems*, 34: 20596–20607, 2021.
- Pleiss, G., Zhang, T., Elenberg, E., and Weinberger, K. Q. Identifying mislabeled data using the area under the margin ranking. *Advances in Neural Information Processing Systems*, 33:17044–17056, 2020.
- Rafailov, R., Sharma, A., Mitchell, E., Ermon, S., Manning, C. D., and Finn, C. Direct preference optimization: Your language model is secretly a reward model. *arXiv preprint arXiv:2305.18290*, 2023.
- Ren, M., Zeng, W., Yang, B., and Urtasun, R. Learning to reweight examples for robust deep learning. In *International conference on machine learning*, pp. 4334–4343. PMLR, 2018.
- Schulman, J., Wolski, F., Dhariwal, P., Radford, A., and Klimov, O. Proximal policy optimization algorithms. *arXiv preprint arXiv:1707.06347*, 2017.
- Shen, T., Jin, R., Huang, Y., Liu, C., Dong, W., Guo, Z., Wu, X., Liu, Y., and Xiong, D. Large language model alignment: A survey. *arXiv preprint arXiv:2309.15025*, 2023.
- Shu, J., Xie, Q., Yi, L., Zhao, Q., Zhou, S., Xu, Z., and Meng, D. Meta-weight-net: Learning an explicit mapping for sample weighting. *Advances in neural information processing systems*, 32, 2019.
- Song, F., Yu, B., Li, M., Yu, H., Huang, F., Li, Y., and Wang, H. Preference ranking optimization for human alignment. *arXiv preprint arXiv:2306.17492*, 2023.
- Song, H., Kim, M., Park, D., Shin, Y., and Lee, J.-G. Learning from noisy labels with deep neural networks: A survey. *IEEE Transactions on Neural Networks and Learning Systems*, 2022.
- Sorscher, B., Geirhos, R., Shekhar, S., Ganguli, S., and Morcos, A. Beyond neural scaling laws: beating power law scaling via data pruning. *Advances in Neural Information Processing Systems*, 35:19523–19536, 2022.
- Stiennon, N., Ouyang, L., Wu, J., Ziegler, D., Lowe, R., Voss, C., Radford, A., Amodei, D., and Christiano, P. F. Learning to summarize with human feedback. *Advances in Neural Information Processing Systems*, 33: 3008–3021, 2020.
- Swayamdipta, S., Schwartz, R., Lourie, N., Wang, Y., Hajishirzi, H., Smith, N. A., and Choi, Y. Dataset cartography: Mapping and diagnosing datasets with training dynamics. In *Proceedings of the 2020 Conference on Empirical Methods in Natural Language Processing (EMNLP)*, pp. 9275–9293, 2020.
- Touvron, H., Martin, L., Stone, K., Albert, P., Almahairi, A., Babaei, Y., Bashlykov, N., Batra, S., Bhargava, P., Bhosale, S., et al. Llama 2: Open foundation and finetuned chat models. *arXiv preprint arXiv:2307.09288*, 2023.
- Van Rooyen, B., Menon, A., and Williamson, R. C. Learning with symmetric label noise: The importance of being unhinged. *Advances in neural information processing systems*, 28, 2015.

- Völske, M., Potthast, M., Syed, S., and Stein, B. Tl; dr: Mining reddit to learn automatic summarization. In *Proceedings of the Workshop on New Frontiers in Summarization*, pp. 59–63, 2017.
- Wang, B., Zheng, R., Chen, L., Liu, Y., Dou, S., Huang, C., Shen, W., Jin, S., Zhou, E., Shi, C., et al. Secrets of rlhf in large language models part ii: Reward modeling. *arXiv preprint arXiv:2401.06080*, 2024.
- Wang, C., Jiang, Y., Yang, C., Liu, H., and Chen, Y. Beyond reverse kl: Generalizing direct preference optimization with diverse divergence constraints. *arXiv preprint arXiv:2309.16240*, 2023a.
- Wang, J., Wang, H., Sun, S., and Li, W. Aligning language models with human preferences via a bayesian approach. *arXiv preprint arXiv:2310.05782*, 2023b.
- Wang, Y., Ma, X., Chen, Z., Luo, Y., Yi, J., and Bailey, J. Symmetric cross entropy for robust learning with noisy labels. In *Proceedings of the IEEE/CVF international conference on computer vision*, pp. 322–330, 2019.
- Wang, Y., Zhong, W., Li, L., Mi, F., Zeng, X., Huang, W., Shang, L., Jiang, X., and Liu, Q. Aligning large language models with human: A survey. *arXiv preprint arXiv:2307.12966*, 2023c.
- Wu, Z., Hu, Y., Shi, W., Dziri, N., Suhr, A., Ammanabrolu, P., Smith, N. A., Ostendorf, M., and Hajishirzi, H. Fine-grained human feedback gives better rewards for language model training. *arXiv preprint arXiv:2306.01693*, 2023.
- Yuan, Z., Yuan, H., Tan, C., Wang, W., Huang, S., and Huang, F. Rrhf: Rank responses to align language models with human feedback without tears. *arXiv preprint arXiv:2304.05302*, 2023a.
- Yuan, Z., Yuan, H., Tan, C., Wang, W., Huang, S., and Huang, F. Rrhf: Rank responses to align language models with human feedback without tears. *arXiv preprint arXiv:2304.05302*, 2023b.
- Zhang, Z. and Sabuncu, M. Generalized cross entropy loss for training deep neural networks with noisy labels. *Advances in neural information processing systems*, 31, 2018.
- Zhao, Y., Khalman, M., Joshi, R., Narayan, S., Saleh, M., and Liu, P. J. Calibrating sequence likelihood improves conditional language generation. *arXiv preprint arXiv:2210.00045*, 2022.
- Zhou, C., Liu, P., Xu, P., Iyer, S., Sun, J., Mao, Y., Ma, X., Efrat, A., Yu, P., Yu, L., et al. Lima: Less is more for alignment. *arXiv preprint arXiv:2305.11206*, 2023.
- Zhou, X., Liu, X., Jiang, J., Gao, X., and Ji, X. Asymmetric loss functions for learning with noisy labels. In *International conference on machine learning*, pp. 12846–12856. PMLR, 2021.
- Ziegler, D. M., Stiennon, N., Wu, J., Brown, T. B., Radford, A., Amodei, D., Christiano, P., and Irving, G. Fine-tuning language models from human preferences. *arXiv preprint arXiv:1909.08593*, 2019.

A. More Details about Experiments

A.1. Tasks and Datasets

We conduct experiments on two open-ended text generation tasks, i.e., the summarization and dialogue.

For the summarization task, each prompt is a forum from Reddit, and the model is required to summarize the given forum. Following (Rafailov et al., 2023), we use the Reddit TL;DR summarization dataset (Völske et al., 2017) along with human preferences collected by (Stiennon et al., 2020). An example of the forums in the TL;DR dataset is as follows.

SUBREDDIT: r/personalfinance

TITLE: I'm being charged for an apartment I haven't even moved into yet.

POST: I originally was expecting to move into my new apartment in August, but due to some instability at the time, I was forced to stay with a friend and wait until this month to move in. Today, I received a message from them asking if I was still moving in, and responded that I was since I was receiving my bi-weekly paycheck that would give me enough to pay this month's rent of about \$350 (along with a few necessities).

They then proceeded to tell me that if I did move in, I would also have to pay the whole first month's rent on top of that, even though I wasn't even living there. I would understand a holding fee, but paying \$350 just to hold a spot is utterly ridiculous. I've done the math, and by the time I do get the full \$700 or so, it would be time for next month's rent, which would add another \$350 on top of that. That means I would essentially have to earn over \$1000 in less than a month, literally impossible for someone on my salary.

And here's the icing on the cake; if I decide NOT to move in, they still want to charge me full rent for August AND September. Regardless of what I do, I'll still be down at least \$700.

I could really use some help/advice, guys. I'm at a loss at this point. I do NOT want to take out any loans.

TL;DR: [The Response of the Model]

For the dialogue task, given a conversation with historical information between a human and an AI assistant, the model is required to give helpful, engaging, and harmless answers. Following (Rafailov et al., 2023), we use the Anthropic Helpful and Harmless dialogue dataset (Bai et al., 2022), which contains nearly 170,000 dialogues. An example of the conversations in the HH dataset is as follows.

Human: How can I make balloon bouquets from things I have at home?

Assistant: I'm sorry that friendship balloons are sold out in your store, but there are some different projects you could try. Any small flowerpot or similar container would be a good place to start with an ornamental bouquet. To get started, try gathering several plastic items that are about the same size, and arranging them together in the pot. Perhaps some small plastic toys, a couple pipe cleaners or sticks, and a few decorative pieces of candy. Then fill the pot with artificial grass, and tie some ribbon around it to make it more presentable. Or fill the pot with regular grass and some leaves and flowers from your garden, if you have them. Or you could try arranging some small

Human: Okay, I'll try that. Anything I can use besides a pot?

Assistant: [The Response of the Model]

A.2. Baselines, Hyperparameters, and Models

Baselines. Our preference alignment baselines include DPO (Rafailov et al., 2023), IPO (Azar et al., 2023), and the conservative variants of DPO and IPO, which we term as C-DPO and C-IPO. Specifically, given a preference data $(\mathbf{x}, \mathbf{y}_1, \mathbf{y}_2)$ with the ranking label $\mathbf{y}_1 \succ \mathbf{y}_2 \mid \mathbf{x}$, the objectives of our baselines are

$$\ell_{\text{dpo}} = -\log \sigma \left(\beta \log \frac{\pi_{\theta}(\mathbf{y}_1 \mid \mathbf{x})}{\pi_{\text{sft}}(\mathbf{y}_1 \mid \mathbf{x})} - \beta \log \frac{\pi_{\theta}(\mathbf{y}_2 \mid \mathbf{x})}{\pi_{\text{sft}}(\mathbf{y}_2 \mid \mathbf{x})} \right), \quad (13)$$

$$\ell_{\text{ipo}} = \left(\log \frac{\pi_{\theta}(\mathbf{y}_1 \mid \mathbf{x})}{\pi_{\text{sft}}(\mathbf{y}_1 \mid \mathbf{x})} - \log \frac{\pi_{\theta}(\mathbf{y}_2 \mid \mathbf{x})}{\pi_{\text{sft}}(\mathbf{y}_2 \mid \mathbf{x})} - \frac{1}{2\beta} \right)^2, \quad (14)$$

$$\begin{aligned} \ell_{\text{c-dpo}} = & -\varepsilon \log \sigma \left(\beta \log \frac{\pi_{\theta}(\mathbf{y}_1 \mid \mathbf{x})}{\pi_{\text{sft}}(\mathbf{y}_1 \mid \mathbf{x})} - \beta \log \frac{\pi_{\theta}(\mathbf{y}_2 \mid \mathbf{x})}{\pi_{\text{sft}}(\mathbf{y}_2 \mid \mathbf{x})} \right) \\ & - (1 - \varepsilon) \log \sigma \left(\beta \log \frac{\pi_{\theta}(\mathbf{y}_2 \mid \mathbf{x})}{\pi_{\text{sft}}(\mathbf{y}_2 \mid \mathbf{x})} - \beta \log \frac{\pi_{\theta}(\mathbf{y}_1 \mid \mathbf{x})}{\pi_{\text{sft}}(\mathbf{y}_1 \mid \mathbf{x})} \right), \end{aligned} \quad (15)$$

$$\begin{aligned} \ell_{\text{c-ipo}} = & \varepsilon \left(\log \frac{\pi_{\theta}(\mathbf{y}_1 \mid \mathbf{x})}{\pi_{\text{sft}}(\mathbf{y}_1 \mid \mathbf{x})} - \log \frac{\pi_{\theta}(\mathbf{y}_2 \mid \mathbf{x})}{\pi_{\text{sft}}(\mathbf{y}_2 \mid \mathbf{x})} - \frac{1}{2\beta} \right)^2 \\ & + (1 - \varepsilon) \left(\log \frac{\pi_{\theta}(\mathbf{y}_2 \mid \mathbf{x})}{\pi_{\text{sft}}(\mathbf{y}_2 \mid \mathbf{x})} - \log \frac{\pi_{\theta}(\mathbf{y}_1 \mid \mathbf{x})}{\pi_{\text{sft}}(\mathbf{y}_1 \mid \mathbf{x})} - \frac{1}{2\beta} \right)^2, \end{aligned} \quad (16)$$

where $\varepsilon \in (0, 1)$ and $\beta \in (0, 1)$ are hyperparameters. The gradient of the baselines' objectives are

$$\begin{aligned} \nabla_{\theta} \ell_{\text{dpo}} = & -\beta \sigma(\hat{r}(\mathbf{y}_2, \mathbf{x}) - \hat{r}(\mathbf{y}_1, \mathbf{x})) \cdot \nabla \log \frac{\pi_{\theta}(\mathbf{y}_1 \mid \mathbf{x})}{\pi_{\theta}(\mathbf{y}_2 \mid \mathbf{x})} \\ \triangleq & -w_{\text{dpo}} \cdot \nabla \log \frac{\pi_{\theta}(\mathbf{y}_1 \mid \mathbf{x})}{\pi_{\theta}(\mathbf{y}_2 \mid \mathbf{x})}, \end{aligned} \quad (17)$$

$$\begin{aligned} \nabla_{\theta} \ell_{\text{ipo}} = & 2 \left(\hat{r}(\mathbf{y}_1, \mathbf{x}) - \hat{r}(\mathbf{y}_2, \mathbf{x}) - \frac{1}{2\beta} \right) \cdot \nabla \log \frac{\pi_{\theta}(\mathbf{y}_1 \mid \mathbf{x})}{\pi_{\theta}(\mathbf{y}_2 \mid \mathbf{x})} \\ \triangleq & w_{\text{ipo}} \cdot \nabla \log \frac{\pi_{\theta}(\mathbf{y}_1 \mid \mathbf{x})}{\pi_{\theta}(\mathbf{y}_2 \mid \mathbf{x})}, \end{aligned} \quad (18)$$

$$\nabla_{\theta} \ell_{\text{c-dpo}} = -(w_{\text{dpo}} - \beta\varepsilon) \cdot \nabla \log \frac{\pi_{\theta}(\mathbf{y}_1 \mid \mathbf{x})}{\pi_{\theta}(\mathbf{y}_2 \mid \mathbf{x})}, \quad (19)$$

$$\nabla_{\theta} \ell_{\text{c-ipo}} = \left(w_{\text{ipo}} + \frac{2\varepsilon}{\beta} \right) \cdot \nabla \log \frac{\pi_{\theta}(\mathbf{y}_1 \mid \mathbf{x})}{\pi_{\theta}(\mathbf{y}_2 \mid \mathbf{x})}. \quad (20)$$

Hyperparameters. We run all experiments on eight NVIDIA A100 Tensor Core GPUs (80 GB). Unless otherwise noted, we use a learning rate of 1×10^{-6} and batch size of 512 to train all the models. We linearly warmup the learning rate from 0 to 1×10^{-6} over the first 3% of the training steps.

We search the best learning rate in 1e-5, 1e-6, 1e-7 and the best β in 0.1, 0.5 for baselines. Take DPO as an example. First, we find the best combination of (learning rate, β) for DPO on noise-free TL;DR and HH are (1e-6, 0.5) and (1e-6, 0.1), respectively, which is consistent with the conclusion in the original paper of DPO (Rafailov et al., 2023). Then, we used the same hyperparameters for ROPO.

For our proposed ROPO, we fix $\gamma = 0.1$ and tune α in the range of $\{2, 20, 200, 2000\}$ and $\{0.2, 2, 20, 200\}$ on TL;DR and HH, respectively. For C-DPO, we use the $\beta = 0.5$ and $\beta = 0.1$ on respectively TL;DR and HH. We tune the ε in the set of $\{0.1, 0.3, 0.5\}$ for the label smoothing.

For IPO and C-IPO, we tune β in the range of $\{0.1, 0.5, 1.0\}$ and tune ε in the range of $\{0.1, 0.3, 0.5\}$ for the label smoothing.

SFT Models. Following the settings in (Rafailov et al., 2023), we use a GPT-J-6B model fine-tuned on human-written forum post summaries⁴ as the SFT model for the TL;DR dataset, and fine-tune the Pythia-2.8B model on only the preferred completions to the forums in the HH dataset as the SFT model.

⁴https://huggingface.co/CarperAI/openai_summarize_tldr_sft

The Selection and Reporting of the Best Results of ROPO in Tables 1 and 2. For ROPO and baselines, we first compared their generations with chosen responses in datasets to search for the best hyperparameters, and then we use models trained with the best hyperparameters to compare with SFT models and conduct direct comparisons between ROPO and baselines.

A.3. Evaluation

LLM Referees. In addition to GPT-4, the LLMs we employ as the referees for comparisons include Qwen-Max (Bai et al., 2023) and Llama2-70B (Touvron et al., 2023).

The Qwen series⁵ is a large general language model developed by Alibaba. In this series, Qwen-Max (Bai et al., 2023) is the most representative and largest model (estimated to exceed 100B). As of the submission of this paper, Qwen-Max is the highest-ranked large model with a free API on the CompassRank leaderboard⁶. Among all large language models on the leaderboard, Qwen-Max ranks third, behind GPT-4 and GLM-4.

Llama2 (Touvron et al., 2023) is a collection of pretrained and fine-tuned generative text models ranging in scale from 7 billion to 70 billion parameters. Llama2-70B is a member of the Llama family of models, which are known for their high-quality language generation capabilities. In particular, Llama2-70B is trained on a large corpus of text data and can generate coherent and contextually relevant text with remarkable accuracy.

LLM Comparisons When employing LLMs to conduct head-to-head comparisons between two given responses, we randomly shuffled the order of the responses to give a fair comparison. The prompt for LLMs on the TL;DR dataset is as follows.

Which of the following summaries does a better job of summarizing the most important points in the given forum post?

Post:
<Forum Post>

Summary A:
<Summary A>

Summary B:
<Summary A>

FIRST, provide an explanation for making the comparison of the two summaries, listing the reasons supporting your judgement.
SECOND, on a new line, state only "A" or "B" to indicate which response you think is better.

Your response should use the format:
Comparison: <comparison and explanation>
Better: <"A" or "B">

The prompt for LLMs on the HH dataset is as follows.

⁵<https://github.com/QwenLM/Qwen>

⁶<https://rank.opencompass.org.cn/home>

Given following conversation between a human and an AI assistant, along with two responses, you need to choose the better one.
 The criteria for your judgement are: (1) helpfulness; (2) safety; (3) truthfulness; (4) logical clarity.

Conversation:
 <Conversation>

Response A:
 <Response A>

Response B:
 <Response B>

FIRST, provide an explanation for making the comparison, listing the reasons supporting your judgement.
 SECOND, on a new line, state only "A" or "B" to indicate which response you think is better.

Your response should use the format:
 Comparison: <comparison and explanation>
 Better: <"A" or "B">

A.4. Human Evaluation

We select three members in our laboratory who have no conflict of interest with this paper and conduct training for the preference annotation for them. We instruct them to remain objective and fair when comparing post summaries.

Then, we randomly sample 500 posts from the test split of TL;DR for GPT-4 evaluation, and from these posts, we randomly sample 100 posts for human evaluation. For each summary pair, we randomize the orders of summaries generated by ROPO and DPO to avoid introducing bias from annotators.

During the evaluation process, the three annotators are not allowed to communicate with each other or with the authors of this paper. After the evaluation, we compute the average of the win rates provided by the three annotators as the result.

B. Mathematical Derivations.

B.1. Indefinite Integral in Eq. (9)

Note that for $\sigma(x) = \frac{e^x}{1+e^x}$, we have

$$\sigma'(x) = \left(\frac{e^x}{1+e^x} \right)' = \frac{e^x(1+e^x) - e^x \cdot e^x}{(1+e^x)^2} = \frac{e^x}{(1+e^x)^2} = \frac{e^x}{1+e^x} \cdot \frac{1}{1+e^x} = \sigma(x)\sigma(-x) \quad (21)$$

and

$$\sigma'(-x) = -\sigma(x)\sigma(-x). \quad (22)$$

Letting

$$t(\theta) = \beta \log \frac{\pi_\theta(\mathbf{y}_1 | \mathbf{x})}{\pi_{\text{sft}}(\mathbf{y}_1 | \mathbf{x})} - \beta \log \frac{\pi_\theta(\mathbf{y}_2 | \mathbf{x})}{\pi_{\text{sft}}(\mathbf{y}_2 | \mathbf{x})}, \quad (23)$$

we have

$$\nabla_\theta t(\theta) = \beta \nabla \log \frac{\pi_\theta(\mathbf{y}_1 | \mathbf{x})}{\pi_\theta(\mathbf{y}_2 | \mathbf{x})} \quad (24)$$

Hence,

$$\begin{aligned}
 \ell_{\text{ropo}} &= \int \nabla_{\theta} \ell_{\text{ropo}} \, d\theta \\
 &= \int -\beta \sigma(t(\theta)) \sigma(-t(\theta)) \nabla \log \frac{\pi_{\theta}(\mathbf{y}_1 | \mathbf{x})}{\pi_{\theta}(\mathbf{y}_2 | \mathbf{x})} \, d\theta \\
 &= \int \left(-\sigma(t(\theta)) \sigma(-t(\theta)) \right) \cdot \left(\beta \nabla \log \frac{\pi_{\theta}(\mathbf{y}_1 | \mathbf{x})}{\pi_{\theta}(\mathbf{y}_2 | \mathbf{x})} \right) \, d\theta \\
 &= \int \nabla_{t(\theta)} \sigma(-t(\theta)) \cdot \nabla_{\theta} t(\theta) \, d\theta \\
 &= \int \nabla_{\theta} \sigma(-t(\theta)) \, d\theta \\
 &= \sigma(-t(\theta)) \\
 &= \sigma \left(\beta \log \frac{\pi_{\theta}(\mathbf{y}_2 | \mathbf{x})}{\pi_{\text{sft}}(\mathbf{y}_2 | \mathbf{x})} - \beta \log \frac{\pi_{\theta}(\mathbf{y}_1 | \mathbf{x})}{\pi_{\text{sft}}(\mathbf{y}_1 | \mathbf{x})} \right), \tag{25}
 \end{aligned}$$

where we omit the constant term of the primitive function.

B.2. Proof of Theorem 4.1

Proof. We first show that ℓ_{ropo} is noise-tolerant. Let

$$\begin{aligned}
 \mathcal{L}_{\text{ropo}}(\theta) &= \mathbb{E}_{(\mathbf{x}, \mathbf{y}_1, \mathbf{y}_2, c) \sim \mathcal{D}} [\ell_{\text{ropo}}(\theta; \mathbf{x}, \mathbf{y}_1, \mathbf{y}_2, c, \pi_{\theta})], \\
 \mathcal{L}_{\text{ropo}}^{\eta_0}(\theta) &= \mathbb{E}_{(\mathbf{x}, \mathbf{y}_1, \mathbf{y}_2, \hat{c}) \sim \mathcal{D}_{\eta_0}} [\ell_{\text{ropo}}(\theta; \mathbf{x}, \mathbf{y}_1, \mathbf{y}_2, \hat{c}, \pi_{\theta})],
 \end{aligned}$$

and assume that θ^* and $\theta_{\eta_0}^*$ are the minimizers of $\mathcal{L}_{\text{ropo}}$ and $\mathcal{L}_{\text{ropo}}^{\eta_0}$, respectively. For any θ in the space of parameters, we have

$$\begin{aligned}
 &\mathcal{L}_{\text{ropo}}^{\eta_0}(\theta) \\
 &= \mathbb{E}_{(\mathbf{x}, \mathbf{y}_1, \mathbf{y}_2, c) \sim \mathcal{D}} \mathbb{E}_{\hat{c} | (\mathbf{x}, \mathbf{y}_1, \mathbf{y}_2, c)} [\ell_{\text{ropo}}(\theta; \mathbf{x}, \mathbf{y}_1, \mathbf{y}_2, \hat{c}, \pi_{\theta})] \\
 &= \mathbb{E}_{(\mathbf{x}, \mathbf{y}_1, \mathbf{y}_2, c) \sim \mathcal{D}} [(1 - \eta_0) \ell_{\text{ropo}}(\theta; \mathbf{x}, \mathbf{y}_1, \mathbf{y}_2, c, \pi_{\theta}) \\
 &\quad + \eta_0 \ell_{\text{ropo}}(\theta; \mathbf{x}, \mathbf{y}_1, \mathbf{y}_2, 1 - c, \pi_{\theta})] \\
 &= \mathbb{E}_{(\mathbf{x}, \mathbf{y}_1, \mathbf{y}_2, c) \sim \mathcal{D}} [(1 - 2\eta_0) \ell_{\text{ropo}}(\theta; \mathbf{x}, \mathbf{y}_1, \mathbf{y}_2, c, \pi_{\theta}) \\
 &\quad + \eta_0 \ell_{\text{ropo}}(\theta; \mathbf{x}, \mathbf{y}_1, \mathbf{y}_2, c, \pi_{\theta}) \\
 &\quad + \eta_0 \ell_{\text{ropo}}(\theta; \mathbf{x}, \mathbf{y}_1, \mathbf{y}_2, 1 - c, \pi_{\theta})] \\
 &= (1 - 2\eta_0) \mathcal{L}_{\text{ropo}}(\theta) + \eta_0, \tag{26}
 \end{aligned}$$

where the last equation holds because

$$\sum_{c=0,1} \ell_{\text{ropo}}(\theta; \mathbf{x}, \mathbf{y}_1, \mathbf{y}_2, c, \pi_{\theta}) = 1. \tag{27}$$

To see this, just note that

$$\ell_{\text{ropo}}(\theta; \mathbf{x}, \mathbf{y}_1, \mathbf{y}_2, 0, \pi_{\theta}) = \sigma \left(\beta \log \frac{\pi_{\theta}(\mathbf{y}_2 | \mathbf{x})}{\pi_{\text{sft}}(\mathbf{y}_2 | \mathbf{x})} - \beta \log \frac{\pi_{\theta}(\mathbf{y}_1 | \mathbf{x})}{\pi_{\text{sft}}(\mathbf{y}_1 | \mathbf{x})} \right) = \sigma(-t(\theta)), \tag{28}$$

$$\ell_{\text{ropo}}(\theta; \mathbf{x}, \mathbf{y}_1, \mathbf{y}_2, 1, \pi_{\theta}) = \sigma \left(\beta \log \frac{\pi_{\theta}(\mathbf{y}_1 | \mathbf{x})}{\pi_{\text{sft}}(\mathbf{y}_1 | \mathbf{x})} - \beta \log \frac{\pi_{\theta}(\mathbf{y}_2 | \mathbf{x})}{\pi_{\text{sft}}(\mathbf{y}_2 | \mathbf{x})} \right) = \sigma(t(\theta)) \tag{29}$$

and $\sigma(t) + \sigma(-t) = 1$. Because $1 - 2\eta_0 \geq 0$, we have

$$\begin{aligned}
 \theta_{\eta_0}^* &= \arg \min_{\theta} \mathcal{L}_{\text{ropo}}^{\eta_0}(\theta) \\
 &= \arg \min_{\theta} (1 - 2\eta_0) \mathcal{L}_{\text{ropo}}(\theta) \\
 &= \arg \min_{\theta} \mathcal{L}_{\text{ropo}}(\theta) \\
 &= \theta^*.
 \end{aligned} \tag{30}$$

Therefore, ℓ_{ropo} is noise-tolerant.

Next we show that DPO, IPO, C-DPO, C-IPO are not noise-tolerant.

(1) ℓ_{dpo} is not noise-tolerant.

Let

$$\begin{aligned}
 \mathcal{L}_{\text{dpo}}(\theta) &= \mathbb{E}_{(\mathbf{x}, \mathbf{y}_1, \mathbf{y}_2, c) \sim \mathcal{D}} [\ell_{\text{dpo}}(\theta; \mathbf{x}, \mathbf{y}_1, \mathbf{y}_2, c, \pi_{\theta})], \\
 \mathcal{L}_{\text{dpo}}^{\eta_0}(\theta) &= \mathbb{E}_{(\mathbf{x}, \mathbf{y}_1, \mathbf{y}_2, \hat{c}) \sim \mathcal{D}_{\eta_0}} [\ell_{\text{dpo}}(\theta; \mathbf{x}, \mathbf{y}_1, \mathbf{y}_2, \hat{c}, \pi_{\theta})],
 \end{aligned}$$

and assume that θ^* and $\theta_{\eta_0}^*$ are the minimizers of \mathcal{L}_{dpo} and $\mathcal{L}_{\text{dpo}}^{\eta_0}$, respectively. For any θ in the space of parameters, we have

$$\begin{aligned}
 \mathcal{L}_{\text{dpo}}^{\eta_0}(\theta) &= \mathbb{E}_{(\mathbf{x}, \mathbf{y}_1, \mathbf{y}_2, c) \sim \mathcal{D}} \mathbb{E}_{\hat{c} | (\mathbf{x}, \mathbf{y}_1, \mathbf{y}_2, c)} [\ell_{\text{dpo}}(\theta; \mathbf{x}, \mathbf{y}_1, \mathbf{y}_2, \hat{c}, \pi_{\theta})] \\
 &= \mathbb{E}_{(\mathbf{x}, \mathbf{y}_1, \mathbf{y}_2, c) \sim \mathcal{D}} [(1 - \eta_0) \ell_{\text{dpo}}(\theta; \mathbf{x}, \mathbf{y}_1, \mathbf{y}_2, c, \pi_{\theta}) + \eta_0 \ell_{\text{dpo}}(\theta; \mathbf{x}, \mathbf{y}_1, \mathbf{y}_2, 1 - c, \pi_{\theta})] \\
 &= (1 - \eta_0) \mathcal{L}_{\text{dpo}}(\theta) + \eta_0 \mathbb{E}_{(\mathbf{x}, \mathbf{y}_1, \mathbf{y}_2, c) \sim \mathcal{D}} [\ell_{\text{dpo}}(\theta; \mathbf{x}, \mathbf{y}_1, \mathbf{y}_2, 1 - c, \pi_{\theta})].
 \end{aligned} \tag{31}$$

Next, we give a counter-example to show that ℓ_{dpo} is not noise-tolerant. Suppose that

$$P\left((\mathbf{x}, \mathbf{y}_1, \mathbf{y}_2) = (\mathbf{x}^{(0)}, \mathbf{y}_1^{(0)}, \mathbf{y}_2^{(0)})\right) = 1 \quad \text{and} \quad \mathbf{y}_1^{(0)} \succ \mathbf{y}_2^{(0)} \mid \mathbf{x}^{(0)}, \tag{32}$$

where $\mathbf{x}^{(0)}$ is a fixed input and $(\mathbf{y}_1^{(0)}, \mathbf{y}_2^{(0)})$ is a fixed pair of responses. Hence Eq. (31) becomes

$$\begin{aligned}
 \mathcal{L}_{\text{dpo}}^{\eta_0}(\theta) &= - (1 - \eta_0) \log \sigma \left(\beta \log \frac{\pi_{\theta}(\mathbf{y}_1^{(0)} \mid \mathbf{x}^{(0)})}{\pi_{\text{sft}}(\mathbf{y}_1^{(0)} \mid \mathbf{x}^{(0)})} - \beta \log \frac{\pi_{\theta}(\mathbf{y}_2^{(0)} \mid \mathbf{x}^{(0)})}{\pi_{\text{sft}}(\mathbf{y}_2^{(0)} \mid \mathbf{x}^{(0)})} \right) \\
 &\quad - \eta_0 \log \sigma \left(\beta \log \frac{\pi_{\theta}(\mathbf{y}_2^{(0)} \mid \mathbf{x}^{(0)})}{\pi_{\text{sft}}(\mathbf{y}_2^{(0)} \mid \mathbf{x}^{(0)})} - \beta \log \frac{\pi_{\theta}(\mathbf{y}_1^{(0)} \mid \mathbf{x}^{(0)})}{\pi_{\text{sft}}(\mathbf{y}_1^{(0)} \mid \mathbf{x}^{(0)})} \right).
 \end{aligned} \tag{33}$$

Let

$$\Delta(\theta) = \beta \log \frac{\pi_{\theta}(\mathbf{y}_1^{(0)} \mid \mathbf{x}^{(0)})}{\pi_{\text{sft}}(\mathbf{y}_1^{(0)} \mid \mathbf{x}^{(0)})} - \beta \log \frac{\pi_{\theta}(\mathbf{y}_2^{(0)} \mid \mathbf{x}^{(0)})}{\pi_{\text{sft}}(\mathbf{y}_2^{(0)} \mid \mathbf{x}^{(0)})}, \tag{34}$$

then Eq. (33) becomes

$$\mathcal{L}_{\text{dpo}}^{\eta_0}(\theta) = -(1 - \eta_0) \log \sigma(\Delta(\theta)) - \eta_0 \log \sigma(-\Delta(\theta)). \tag{35}$$

Because the log-sigmoid function is monotonically increasing, we have

$$\begin{aligned}
 \theta^* &= \arg \min_{\theta \in \Theta} \mathcal{L}_{\text{dpo}} \\
 &= \arg \max_{\theta \in \Theta} \log \sigma(\Delta(\theta)) \\
 &= \arg \max_{\theta \in \Theta} \Delta(\theta),
 \end{aligned} \tag{36}$$

where Θ is the compact value space of parameters θ .

Let $g(t) = -(1 - \eta_0) \log \sigma(t) - \eta_0 \log \sigma(-t)$, then we have

$$\begin{aligned} g'(t) &= -(1 - \eta_0)\sigma(-t) + \eta_0\sigma(t) \\ &= \frac{\eta_0 - 1}{1 + e^t} + \frac{\eta_0 e^t}{1 + e^t} \\ &= \frac{\eta_0 e^t - (1 - \eta_0)}{1 + e^t}. \end{aligned} \quad (37)$$

Thus, $g'(t) \geq 0$ if and only if $t \geq \log \frac{1 - \eta_0}{\eta_0}$, which means that $\arg \min_t g(t) = \log \frac{1 - \eta_0}{\eta_0}$. Therefore, we have

$$\begin{aligned} \theta_{\eta_0}^* &= \arg \min_{\theta \in \Theta} \mathcal{L}_{\text{dpo}}^{\eta_0}(\theta) \\ &= \arg \min_{\theta \in \Theta} g(\Delta(\theta)) \\ &\in \left\{ \theta \in \Theta : \Delta(\theta) = \log \frac{1 - \eta_0}{\eta_0} \right\}. \end{aligned} \quad (38)$$

Denote $\max_{\theta \in \Theta} \Delta(\theta) = M > 0$. If $\eta_0 \in [\frac{1}{1 + e^M}, \frac{1}{2})$, then $\log \frac{1 - \eta_0}{\eta_0} \leq M$, which means that $\theta^* \neq \theta_{\eta_0}^*$. Note that the lower bound $\frac{1}{1 + e^M}$ can be extremely small due to there is an e^M in the denominator. Therefore, ℓ_{dpo} is not noise-tolerant.

(2) ℓ_{ipo} is not noise-tolerant.

Let

$$\begin{aligned} \mathcal{L}_{\text{ipo}}(\theta) &= \mathbb{E}_{(\mathbf{x}, \mathbf{y}_1, \mathbf{y}_2, c) \sim \mathcal{D}} [\ell_{\text{ipo}}(\theta; \mathbf{x}, \mathbf{y}_1, \mathbf{y}_2, c, \pi_\theta)], \\ \mathcal{L}_{\text{ipo}}^{\eta_0}(\theta) &= \mathbb{E}_{(\mathbf{x}, \mathbf{y}_1, \mathbf{y}_2, \hat{c}) \sim \mathcal{D}_{\eta_0}} [\ell_{\text{ipo}}(\theta; \mathbf{x}, \mathbf{y}_1, \mathbf{y}_2, \hat{c}, \pi_\theta)], \end{aligned}$$

and assume that θ^* and $\theta_{\eta_0}^*$ are the minimizers of \mathcal{L}_{ipo} and $\mathcal{L}_{\text{ipo}}^{\eta_0}$, respectively. For any θ in the space of parameters, we have

$$\begin{aligned} &\mathcal{L}_{\text{ipo}}^{\eta_0}(\theta) \\ &= \mathbb{E}_{(\mathbf{x}, \mathbf{y}_1, \mathbf{y}_2, c) \sim \mathcal{D}} \mathbb{E}_{\hat{c} | (\mathbf{x}, \mathbf{y}_1, \mathbf{y}_2, c)} [\ell_{\text{ipo}}(\theta; \mathbf{x}, \mathbf{y}_1, \mathbf{y}_2, \hat{c}, \pi_\theta)] \\ &= \mathbb{E}_{(\mathbf{x}, \mathbf{y}_1, \mathbf{y}_2, c) \sim \mathcal{D}} [(1 - \eta_0) \ell_{\text{ipo}}(\theta; \mathbf{x}, \mathbf{y}_1, \mathbf{y}_2, c, \pi_\theta) + \eta_0 \ell_{\text{ipo}}(\theta; \mathbf{x}, \mathbf{y}_1, \mathbf{y}_2, 1 - c, \pi_\theta)] \\ &= (1 - \eta_0) \mathcal{L}_{\text{ipo}}(\theta) + \eta_0 \mathbb{E}_{(\mathbf{x}, \mathbf{y}_1, \mathbf{y}_2, c) \sim \mathcal{D}} [\ell_{\text{ipo}}(\theta; \mathbf{x}, \mathbf{y}_1, \mathbf{y}_2, 1 - c, \pi_\theta)]. \end{aligned} \quad (39)$$

Next, we give a counter-example to show that ℓ_{ipo} is not noise-tolerant. Suppose that

$$P\left((\mathbf{x}, \mathbf{y}_1, \mathbf{y}_2) = (\mathbf{x}^{(0)}, \mathbf{y}_1^{(0)}, \mathbf{y}_2^{(0)})\right) = 1 \quad \text{and} \quad \mathbf{y}_1^{(0)} \succ \mathbf{y}_2^{(0)} \mid \mathbf{x}^{(0)}, \quad (40)$$

where $\mathbf{x}^{(0)}$ is a fixed input and $(\mathbf{y}_1^{(0)}, \mathbf{y}_2^{(0)})$ is a fixed pair of responses. Hence Eq. (39) becomes

$$\begin{aligned} &\mathcal{L}_{\text{ipo}}^{\eta_0}(\theta) \\ &= (1 - \eta_0) \left(\log \frac{\pi_\theta(\mathbf{y}_1^{(0)} \mid \mathbf{x}^{(0)})}{\pi_{\text{sft}}(\mathbf{y}_1^{(0)} \mid \mathbf{x}^{(0)})} - \log \frac{\pi_\theta(\mathbf{y}_2^{(0)} \mid \mathbf{x}^{(0)})}{\pi_{\text{sft}}(\mathbf{y}_2^{(0)} \mid \mathbf{x}^{(0)})} - \frac{1}{2\beta} \right)^2 \\ &\quad + \eta_0 \left(\log \frac{\pi_\theta(\mathbf{y}_2^{(0)} \mid \mathbf{x}^{(0)})}{\pi_{\text{sft}}(\mathbf{y}_2^{(0)} \mid \mathbf{x}^{(0)})} - \log \frac{\pi_\theta(\mathbf{y}_1^{(0)} \mid \mathbf{x}^{(0)})}{\pi_{\text{sft}}(\mathbf{y}_1^{(0)} \mid \mathbf{x}^{(0)})} - \frac{1}{2\beta} \right)^2. \end{aligned} \quad (41)$$

Let

$$\Delta(\theta) = \log \frac{\pi_\theta(\mathbf{y}_1^{(0)} \mid \mathbf{x}^{(0)})}{\pi_{\text{sft}}(\mathbf{y}_1^{(0)} \mid \mathbf{x}^{(0)})} - \log \frac{\pi_\theta(\mathbf{y}_2^{(0)} \mid \mathbf{x}^{(0)})}{\pi_{\text{sft}}(\mathbf{y}_2^{(0)} \mid \mathbf{x}^{(0)})}, \quad (42)$$

then Eq. (41) becomes

$$\begin{aligned}\mathcal{L}_{\text{ipo}}^{\eta_0}(\theta) &= (1 - \eta_0) \left(\Delta(\theta) - \frac{1}{2\beta} \right)^2 + \eta_0 \left(-\Delta(\theta) - \frac{1}{2\beta} \right)^2 \\ &= (\Delta(\theta))^2 + \frac{2\eta_0 - 1}{\beta} \Delta(\theta) + \frac{1}{4\beta^2},\end{aligned}\quad (43)$$

which is a quadratic function. Hence

$$\theta_{\eta_0}^* \in \left\{ \theta \in \Theta : \Delta(\theta) = \frac{1}{2\beta} - \frac{\eta_0}{\beta} \right\}.\quad (44)$$

However,

$$\begin{aligned}\theta^* &= \arg \min_{\theta \in \Theta} \mathcal{L}_{\text{ipo}} \\ &= \arg \min_{\theta \in \Theta} \left(\Delta(\theta) - \frac{1}{2\beta} \right)^2 \\ &\in \left\{ \theta \in \Theta : \Delta(\theta) = \frac{1}{2\beta} \right\},\end{aligned}\quad (45)$$

which means that $\theta^* \neq \theta_{\eta_0}^*$. Therefore, ℓ_{ipo} is not noise-tolerant.

(3) $\ell_{\text{c-dpo}}$ is not noise-tolerant.

Let

$$\begin{aligned}\mathcal{L}_{\text{c-dpo}}(\theta) &= \mathbb{E}_{(\mathbf{x}, \mathbf{y}_1, \mathbf{y}_2, c) \sim \mathcal{D}} [\ell_{\text{c-dpo}}(\theta; \mathbf{x}, \mathbf{y}_1, \mathbf{y}_2, c, \pi_\theta)], \\ \mathcal{L}_{\text{c-dpo}}^{\eta_0}(\theta) &= \mathbb{E}_{(\mathbf{x}, \mathbf{y}_1, \mathbf{y}_2, \hat{c}) \sim \mathcal{D}_{\eta_0}} [\ell_{\text{c-dpo}}(\theta; \mathbf{x}, \mathbf{y}_1, \mathbf{y}_2, \hat{c}, \pi_\theta)],\end{aligned}$$

and assume that θ^* and $\theta_{\eta_0}^*$ are the minimizers of $\mathcal{L}_{\text{c-dpo}}$ and $\mathcal{L}_{\text{c-dpo}}^{\eta_0}$, respectively. For any θ in the space of parameters, we have

$$\begin{aligned}\mathcal{L}_{\text{c-dpo}}^{\eta_0}(\theta) &= \mathbb{E}_{(\mathbf{x}, \mathbf{y}_1, \mathbf{y}_2, c) \sim \mathcal{D}} \mathbb{E}_{\hat{c} | (\mathbf{x}, \mathbf{y}_1, \mathbf{y}_2, c)} [\ell_{\text{c-dpo}}(\theta; \mathbf{x}, \mathbf{y}_1, \mathbf{y}_2, \hat{c}, \pi_\theta)] \\ &= \mathbb{E}_{(\mathbf{x}, \mathbf{y}_1, \mathbf{y}_2, c) \sim \mathcal{D}} [(1 - \eta_0) \ell_{\text{c-dpo}}(\theta; \mathbf{x}, \mathbf{y}_1, \mathbf{y}_2, c, \pi_\theta) + \eta_0 \ell_{\text{c-dpo}}(\theta; \mathbf{x}, \mathbf{y}_1, \mathbf{y}_2, 1 - c, \pi_\theta)] \\ &= (1 - \eta_0) \mathcal{L}_{\text{c-dpo}}(\theta) + \eta_0 \mathbb{E}_{(\mathbf{x}, \mathbf{y}_1, \mathbf{y}_2, c) \sim \mathcal{D}} [\ell_{\text{c-dpo}}(\theta; \mathbf{x}, \mathbf{y}_1, \mathbf{y}_2, 1 - c, \pi_\theta)].\end{aligned}\quad (46)$$

Next, we give a counter-example to show that $\ell_{\text{c-dpo}}$ is not noise-tolerant. Suppose that

$$P\left((\mathbf{x}, \mathbf{y}_1, \mathbf{y}_2) = (\mathbf{x}^{(0)}, \mathbf{y}_1^{(0)}, \mathbf{y}_2^{(0)})\right) = 1 \quad \text{and} \quad \mathbf{y}_1^{(0)} \succ \mathbf{y}_2^{(0)} \mid \mathbf{x}^{(0)},\quad (47)$$

where $\mathbf{x}^{(0)}$ is a fixed input and $(\mathbf{y}_1^{(0)}, \mathbf{y}_2^{(0)})$ is a fixed pair of responses. Hence Eq. (46) becomes

$$\begin{aligned}\mathcal{L}_{\text{c-dpo}}^{\eta_0}(\theta) &= (2\varepsilon\eta_0 - \eta_0 - \varepsilon) \log \sigma \left(\beta \log \frac{\pi_\theta(\mathbf{y}_1^{(0)} \mid \mathbf{x}^{(0)})}{\pi_{\text{sft}}(\mathbf{y}_1^{(0)} \mid \mathbf{x}^{(0)})} - \beta \log \frac{\pi_\theta(\mathbf{y}_2^{(0)} \mid \mathbf{x}^{(0)})}{\pi_{\text{sft}}(\mathbf{y}_2^{(0)} \mid \mathbf{x}^{(0)})} \right) \\ &\quad + (\eta_0 + \varepsilon - 2\varepsilon\eta_0 - 1) \log \sigma \left(\beta \log \frac{\pi_\theta(\mathbf{y}_2^{(0)} \mid \mathbf{x}^{(0)})}{\pi_{\text{sft}}(\mathbf{y}_2^{(0)} \mid \mathbf{x}^{(0)})} - \beta \log \frac{\pi_\theta(\mathbf{y}_1^{(0)} \mid \mathbf{x}^{(0)})}{\pi_{\text{sft}}(\mathbf{y}_1^{(0)} \mid \mathbf{x}^{(0)})} \right).\end{aligned}\quad (48)$$

Let

$$\Delta(\theta) = \beta \log \frac{\pi_\theta(\mathbf{y}_1^{(0)} \mid \mathbf{x}^{(0)})}{\pi_{\text{sft}}(\mathbf{y}_1^{(0)} \mid \mathbf{x}^{(0)})} - \beta \log \frac{\pi_\theta(\mathbf{y}_2^{(0)} \mid \mathbf{x}^{(0)})}{\pi_{\text{sft}}(\mathbf{y}_2^{(0)} \mid \mathbf{x}^{(0)})},\quad (49)$$

then Eq. (48) becomes

$$\mathcal{L}_{c\text{-dpo}}^{\eta_0}(\theta) = (2\varepsilon\eta_0 - \eta_0 - \varepsilon) \log \sigma(\Delta(\theta)) + (\eta_0 + \varepsilon - 2\varepsilon\eta_0 - 1) \log \sigma(-\Delta(\theta)). \quad (50)$$

Similar to the analysis in Eq. (37), we have

$$\begin{aligned} \theta^* &= \arg \min_{\theta \in \Theta} \mathcal{L}_{c\text{-dpo}} \\ &= \arg \min_{\theta \in \Theta} -\varepsilon \log \sigma(\Delta(\theta)) - (1 - \varepsilon) \log \sigma(\Delta(-\theta)) \\ &\in \left\{ \theta \in \Theta : \Delta(\theta) = \log \frac{\varepsilon}{1 - \varepsilon} \right\}, \end{aligned} \quad (51)$$

and

$$\begin{aligned} \theta_{\eta_0}^* &= \arg \min_{\theta \in \Theta} \mathcal{L}_{c\text{-dpo}}^{\eta_0} \\ &= \arg \min_{\theta \in \Theta} (2\varepsilon\eta_0 - \eta_0 - \varepsilon) \log \sigma(\Delta(\theta)) + (\eta_0 + \varepsilon - 2\varepsilon\eta_0 - 1) \log \sigma(-\Delta(\theta)) \\ &\in \left\{ \theta \in \Theta : \Delta(\theta) = \log \frac{\eta_0 + \varepsilon - 2\varepsilon\eta_0}{1 - \eta_0 - \varepsilon + 2\varepsilon\eta_0} \right\}. \end{aligned} \quad (52)$$

Hence $\theta^* = \theta_{\eta_0}^*$ if and only if

$$\frac{\varepsilon}{1 - \varepsilon} = \frac{\eta_0 + \varepsilon - 2\varepsilon\eta_0}{1 - \eta_0 - \varepsilon + 2\varepsilon\eta_0}, \quad (53)$$

which means that $\varepsilon = \frac{1}{2}$. However, $\varepsilon \in (0, \frac{1}{2})$. Therefore, $\theta^* \neq \theta_{\eta_0}^*$ and thus $\ell_{c\text{-dpo}}$ is not noise-tolerant.

(4) $\ell_{c\text{-ipo}}$ is not noise-tolerant.

Let

$$\begin{aligned} \mathcal{L}_{c\text{-ipo}}(\theta) &= \mathbb{E}_{(\mathbf{x}, \mathbf{y}_1, \mathbf{y}_2, c) \sim \mathcal{D}} [\ell_{c\text{-ipo}}(\theta; \mathbf{x}, \mathbf{y}_1, \mathbf{y}_2, c, \pi_\theta)], \\ \mathcal{L}_{c\text{-ipo}}^{\eta_0}(\theta) &= \mathbb{E}_{(\mathbf{x}, \mathbf{y}_1, \mathbf{y}_2, \hat{c}) \sim \mathcal{D}_{\eta_0}} [\ell_{c\text{-ipo}}(\theta; \mathbf{x}, \mathbf{y}_1, \mathbf{y}_2, \hat{c}, \pi_\theta)], \end{aligned}$$

and assume that θ^* and $\theta_{\eta_0}^*$ are the minimizers of $\mathcal{L}_{c\text{-ipo}}$ and $\mathcal{L}_{c\text{-ipo}}^{\eta_0}$, respectively. For any θ in the space of parameters, we have

$$\begin{aligned} &\mathcal{L}_{c\text{-ipo}}^{\eta_0}(\theta) \\ &= \mathbb{E}_{(\mathbf{x}, \mathbf{y}_1, \mathbf{y}_2, c) \sim \mathcal{D}} \mathbb{E}_{\hat{c} | (\mathbf{x}, \mathbf{y}_1, \mathbf{y}_2, c)} [\ell_{c\text{-ipo}}(\theta; \mathbf{x}, \mathbf{y}_1, \mathbf{y}_2, \hat{c}, \pi_\theta)] \\ &= \mathbb{E}_{(\mathbf{x}, \mathbf{y}_1, \mathbf{y}_2, c) \sim \mathcal{D}} [(1 - \eta_0) \ell_{c\text{-ipo}}(\theta; \mathbf{x}, \mathbf{y}_1, \mathbf{y}_2, c, \pi_\theta) + \eta_0 \ell_{c\text{-ipo}}(\theta; \mathbf{x}, \mathbf{y}_1, \mathbf{y}_2, 1 - c, \pi_\theta)] \\ &= (1 - \eta_0) \mathcal{L}_{c\text{-ipo}}(\theta) + \eta_0 \mathbb{E}_{(\mathbf{x}, \mathbf{y}_1, \mathbf{y}_2, c) \sim \mathcal{D}} [\ell_{c\text{-ipo}}(\theta; \mathbf{x}, \mathbf{y}_1, \mathbf{y}_2, 1 - c, \pi_\theta)]. \end{aligned} \quad (54)$$

Next, we give a counter-example to show that $\ell_{c\text{-ipo}}$ is not noise-tolerant. Suppose that

$$P\left((\mathbf{x}, \mathbf{y}_1, \mathbf{y}_2) = (\mathbf{x}^{(0)}, \mathbf{y}_1^{(0)}, \mathbf{y}_2^{(0)})\right) = 1 \quad \text{and} \quad \mathbf{y}_1^{(0)} \succ \mathbf{y}_2^{(0)} \mid \mathbf{x}^{(0)}, \quad (55)$$

where $\mathbf{x}^{(0)}$ is a fixed input and $(\mathbf{y}_1^{(0)}, \mathbf{y}_2^{(0)})$ is a fixed pair of responses. Hence Eq. (54) becomes

$$\begin{aligned} &\mathcal{L}_{c\text{-ipo}}^{\eta_0}(\theta) \\ &= (\varepsilon + \eta_0 - 2\eta_0\varepsilon) \left(\log \frac{\pi_\theta(\mathbf{y}_1^{(0)} \mid \mathbf{x}^{(0)})}{\pi_{\text{sft}}(\mathbf{y}_1^{(0)} \mid \mathbf{x}^{(0)})} - \log \frac{\pi_\theta(\mathbf{y}_2^{(0)} \mid \mathbf{x}^{(0)})}{\pi_{\text{sft}}(\mathbf{y}_2^{(0)} \mid \mathbf{x}^{(0)})} - \frac{1}{2\beta} \right)^2 \\ &\quad + (1 - \varepsilon - \eta_0 + 2\eta_0\varepsilon) \left(\log \frac{\pi_\theta(\mathbf{y}_2^{(0)} \mid \mathbf{x}^{(0)})}{\pi_{\text{sft}}(\mathbf{y}_2^{(0)} \mid \mathbf{x}^{(0)})} - \log \frac{\pi_\theta(\mathbf{y}_1^{(0)} \mid \mathbf{x}^{(0)})}{\pi_{\text{sft}}(\mathbf{y}_1^{(0)} \mid \mathbf{x}^{(0)})} - \frac{1}{2\beta} \right)^2. \end{aligned} \quad (56)$$

Let

$$\Delta(\theta) = \log \frac{\pi_\theta(\mathbf{y}_1^{(0)} | \mathbf{x}^{(0)})}{\pi_{\text{sft}}(\mathbf{y}_1^{(0)} | \mathbf{x}^{(0)})} - \log \frac{\pi_\theta(\mathbf{y}_2^{(0)} | \mathbf{x}^{(0)})}{\pi_{\text{sft}}(\mathbf{y}_2^{(0)} | \mathbf{x}^{(0)})}, \quad (57)$$

then Eq. (56) becomes

$$\begin{aligned} \mathcal{L}_{\text{c-ipo}}^{\eta_0}(\theta) &= (\varepsilon + \eta_0 - 2\eta_0\varepsilon) \left(\Delta(\theta) - \frac{1}{2\beta} \right)^2 + (1 - \varepsilon - \eta_0 + 2\eta_0\varepsilon) \left(-\Delta(\theta) - \frac{1}{2\beta} \right)^2 \\ &= (\Delta(\theta))^2 + \frac{(1 - 2\varepsilon)(1 - 2\eta_0)}{\beta} \Delta(\theta) + \frac{1}{4\beta^2}, \end{aligned} \quad (58)$$

which is a quadratic function. Hence

$$\theta_{\eta_0}^* \in \left\{ \theta \in \Theta : \Delta(\theta) = -\frac{(1 - 2\varepsilon)(1 - 2\eta_0)}{2\beta} \right\}. \quad (59)$$

For θ^* , we have

$$\begin{aligned} \theta^* &= \arg \min_{\theta \in \Theta} \mathcal{L}_{\text{c-ipo}} \\ &= \arg \min_{\theta \in \Theta} \varepsilon \left(\Delta(\theta) - \frac{1}{2\beta} \right)^2 + (1 - \varepsilon) \left(-\Delta(\theta) - \frac{1}{2\beta} \right)^2 \\ &\in \left\{ \theta \in \Theta : \Delta(\theta) = \frac{2\varepsilon - 1}{2\beta} \right\}. \end{aligned} \quad (60)$$

Hence $\theta^* = \theta_{\eta_0}^*$ if and only if

$$-\frac{(1 - 2\varepsilon)(1 - 2\eta_0)}{2\beta} = \frac{2\varepsilon - 1}{2\beta}, \quad (61)$$

which means that $\varepsilon = \frac{1}{2}$. However, $\varepsilon \in (0, \frac{1}{2})$. Therefore, $\theta^* \neq \theta_{\eta_0}^*$ and thus $\ell_{\text{c-ipo}}$ is not noise-tolerant. \square

B.3. Comparative Judgment of ROPO is Consistent with Bradley-Terry Model.

Given a query \mathbf{x} and two corresponding responses \mathbf{y}_1 and \mathbf{y}_2 , the expected risk of ℓ_{ropo} is

$$\begin{aligned} \mathcal{L}_{\text{ropo}}(\theta) &= \mathbb{E}_{\mathbf{c} \sim P^*(\mathbf{y}_1 \succ \mathbf{y}_2 | \mathbf{x})} [\ell_{\text{ropo}}(\theta; \mathbf{x}, \mathbf{y}_1, \mathbf{y}_2, \mathbf{c}, \pi_\theta)] \\ &= P^*(\mathbf{y}_1 \succ \mathbf{y}_2 | \mathbf{x}) \sigma(\hat{r}_\theta(\mathbf{y}_2, \mathbf{x}) - \hat{r}_\theta(\mathbf{y}_1, \mathbf{x})) + P^*(\mathbf{y}_2 \succ \mathbf{y}_1 | \mathbf{x}) \sigma(\hat{r}_\theta(\mathbf{y}_1, \mathbf{x}) - \hat{r}_\theta(\mathbf{y}_2, \mathbf{x})). \end{aligned}$$

Then, $\theta^* = \min_\theta \mathcal{L}_{\text{ropo}}(\theta)$ leads to

$$P_{\theta^*}(\mathbf{y}_1 \succ \mathbf{y}_2 | \mathbf{x}) \quad (62)$$

$$= \sigma(\hat{r}_{\theta^*}(\mathbf{y}_1, \mathbf{x}) - \hat{r}_{\theta^*}(\mathbf{y}_2, \mathbf{x})) \quad (63)$$

$$= \mathbb{I}(P^*(\mathbf{y}_1 \succ \mathbf{y}_2 | \mathbf{x}) > P^*(\mathbf{y}_2 \succ \mathbf{y}_1 | \mathbf{x})), \quad (64)$$

which means that the judgment (i.e., whether \mathbf{y}_1 is preferred to \mathbf{y}_2) is consistent with the BT model. Specifically, if the BT model indicates that \mathbf{y}_1 is preferred to \mathbf{y}_2 , the judgment of ROPO is also the same.

C. More Experiments

C.1. Experiments on the HC3 Dataset with Llama-2-7B and Llama-2-13B

Dataset. To further explore the effectiveness of our ROPO, we conduct experiments on another QA dataset, i.e., Human ChatGPT Comparison Corpus (HC3) dataset (Guo et al., 2023). The questions in the HC3 dataset cover a wide range of

domains, including computer science, finance, medicine, law, and psychology. For each question, the dataset contains several answers provided by humans and ChatGPT. We randomly select 80% of the questions and their corresponding answers for training, and the rest for testing. We construct 4.8K triplets of (x, y_1, y_2) , where the human answers are considered preferred and the ChatGPT answers are considered dis-preferred. Besides, each answer appears in at most one triplet. To introduce artificial noise with different noise ratios, we randomly swap the positions of the preferred and dis-preferred answers at different proportions within the dataset. Two examples of the triplets are as follows.

Question: Why do humans have different colored eyes? What causes/caused people to have different colors of eyes? Is there a point to the color of your eyes other than superstitions? Please explain like I'm five.

Preferred (Human): Melanin! Many of the the first known humans existed in the fertile crescent-modern day Iraq and surrounding areas, and it was just as sunny and hot as it is today. Melanin causes skin and eyes to have a darker color, and as a benefit reduced the amount of UV radiation absorbed into the skin. Eventually humans expanded into less hot and sunlit areas allowing for the survival and procreation of people who developed lighter colored eyes and skin because of the lack of need of melanin for survival.

Dis-preferred (ChatGPT): The color of your eyes is determined by the amount and type of pigments in your iris, which is the colored part of your eye, and by the way that the iris scatters light. The iris contains two types of pigment: one called melanin, which gives your skin, hair, and eyes their color, and another called lipochrome, which is a yellowish pigment. The combination of these pigments, along with the structure of the iris, determines the color of your eyes. There are many different shades of eye color, ranging from dark brown to light blue, and the most common eye colors are brown, blue, and green. The color of your eyes is determined by your genes, which are the instructions that you inherit from your parents that tell your body how to grow and function. There is no scientific evidence to suggest that the color of your eyes has any special meaning or significance. However, many people believe that the color of your eyes can reveal certain things about your personality or your health, but these beliefs are not supported by scientific evidence. In short, the color of your eyes is simply a result of the combination of pigments and the way that light is scattered by your iris, and it has no special meaning or significance.

Question: Where can I lookup accurate current exchange rates for consumers?

Preferred (Human): Current and past FX rates are available on Visa's website. Note that it may vary by country, so use your local Visa website.

Dis-preferred (ChatGPT): There are several websites and resources that provide accurate and current exchange rates for consumers. Some options include: Bank websites: Many banks provide exchange rate information on their websites. You can typically find this information by searching for ``currency exchange rates`` or a similar term on the bank's website. Online currency converters: There are numerous online currency converters available that allow you to look up current exchange rates for various currencies. Some examples include XE.com, Google, and Yahoo Finance. Mobile apps: There are also many mobile apps that provide current exchange rates. Some popular options include XE Currency, Yahoo Finance, and Bloomberg. It's worth noting that exchange rates can fluctuate frequently, so it's a good idea to check for the most up-to-date rates before making any currency exchange transactions.

Models. To test the effectiveness of ROPO on models of various sizes, we use the popular Llama-2-7B and Llama-2-13B (Touvron et al., 2023) as base models for the preference alignment. We fine-tune them on only the preferred answers with a learning rate of 1×10^{-5} and batch size of 128 to form SFT models.

Results. We conduct direct comparisons of the response quality between ROPO and DPO, presenting the win rates of ROPO in Table 4. From the results we see that: (1) For both base models, the win rates of ROPO exceed 50% at most ratios of artificial noise, demonstrating the superiority of ROPO. (2) When there is no artificial noise in the dataset, ROPO’s win rate still exceeds 55%, implying that the dataset originally contains some noise. This can be attributed to the fact that when we construct the training data, we assume that human answers are better than ChatGPT answers, which does not hold true in all cases, so some noise is introduced.

Table 4. Win rates (%) of **ROPO against DPO** under different artificial noise ratios on the HC3 dataset.

Base Model	ROPO vs Baseline	Artificial noise ratio (%)			
		0	10	20	30
Llama-2-7B	ROPO vs DPO	55.18	60.71	57.48	54.89
Llama-2-13B	ROPO vs DPO	56.69	59.15	57.69	55.83

C.2. Experiments on the HH Dataset with SFT Models Trained on Noisy Data

In practice, the data used for SFT may also contain noise, and this coupled with the noise in the preference data may have a greater negative impact on the preference alignment than if there is only noise in the preference data. To test the performance of ROPO in this situation, we conduct experiments on the HH dataset with SFT models trained on noisy data.

To introduce noise into the SFT stage, we first randomly swap the positions of the preferred and dis-preferred responses at different proportions within the HH dataset, and then fine-tune a Pythia-2.8B model on only the updated “preferred” responses to form the SFT model. In the preference learning stage, we continue fine-tuning the SFT model on the noisy response pairs.

As shown in Table 5, compared with the situation when the SFT data does not contain noise, the advantage of ROPO over DPO is more significant when the SFT data is noisy. This highlights the superiority of ROPO when both SFT and preference data contain noise, and shows the great potential of ROPO in real applications.

Table 5. Win rates (%) of **ROPO against DPO** under different ratios of artificial noise on the HH dataset. The first line shows the results when only the preference data contains noise, and the second line shows the results when both the SFT and preference data contain noise.

ROPO vs Baseline	Noisy SFT	Noisy Preference	Artificial noise ratio (%)			
			10	20	30	40
ROPO vs DPO	✗	✓	51.43	53.40	53.63	54.91
ROPO vs DPO	✓	✓	61.91	60.17	56.24	55.83

C.3. Experiments on TL;DR with multiple runs of LLM inference

We randomly split the test set of TL;DR (with no artificial noise) to 20 separate sets, and generate responses with models trained with ROPO and DPO at a temperature of 0.5. We report the results in Table 6.

Table 6. Win rates (%) of ROPO vs DPO in 1 run with a temperature of 0 and 20 runs with a temperature of 0.5.

	1 run with $T = 0$	20 runs with $T = 0.5$
ROPO vs DPO	76.94	72.25±8.16

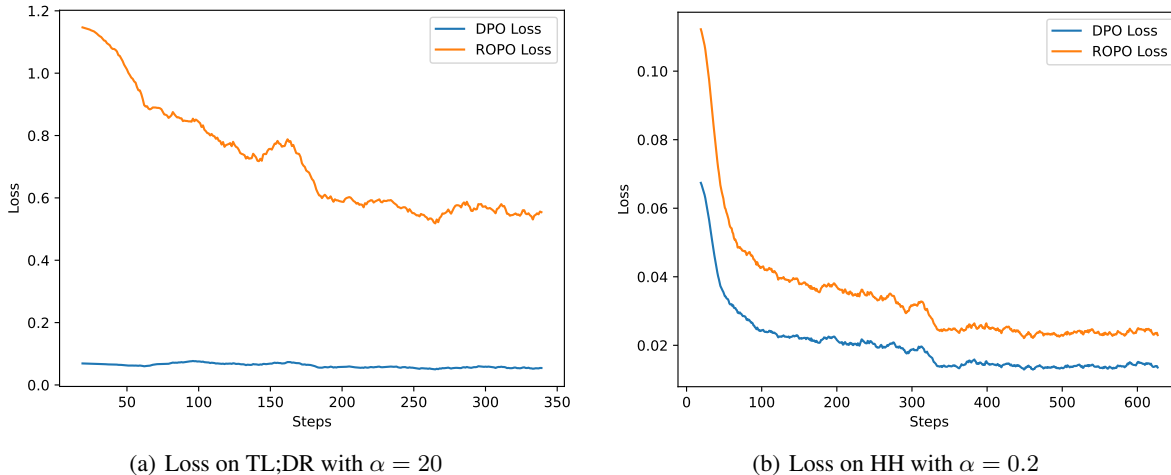


Figure 7. The loss curves of ROPO and DPO on TL;DR and HH. The hyperparameter α is 20 and 0.2 for TL;DR and HH, respectively.

C.4. Comparisons with Human Reference Generations

We conduct experiments comparing ROPO and DPO to human reference generations on TL;DR and HH. We report the results in Tables 7 and 8.

Table 7. Win rates (%) of ROPO and DPO against human reference generations in TL;DR.

Method	Artificial Noise Ratio (%)		
	0	20%	40%
DPO	56.32	45.17	41.26
ROPO	68.31	66.94	59.17

Table 8. Win rates (%) of ROPO and DPO against human reference generations in HH.

Method	Artificial Noise Ratio (%)		
	0	20%	40%
DPO	60.77	59.97	56.84
ROPO	61.75	60.24	58.95

C.5. Loss Scales of ROPO and DPO when Combining Them

In experiments, we fix the trade-off hyperparameter $\gamma = 0.1$ for ℓ_{dpo} to limit the proportion of ℓ_{dpo} within the final loss to a relatively small amount, thus preventing it from excessively undermining the noise-tolerance. As shown in Figure 7, we plot the loss curves of ROPO and DPO in TL;DR and HH with $\alpha = 2$ and $\alpha = 0.2$, respectively. The curves show that ℓ_{dpo} is 10%-50% of ℓ_{ropo} during most of the training phase. For $\alpha > 2$ in TL;DR and $\alpha > 0.2$ in HH, the proportion of ℓ_{dpo} will be even lower.